FINAL REPORT
CHS CONTRACT 06-146
GPS AT SEA FOR HYDROGRAPHIC SURVEYING

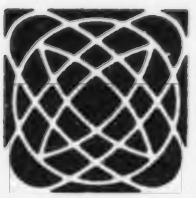

Nortech Surveys

FINAL REPORT
CHS CONTRACT 06-146
GPS AT SEA FOR HYDROGRAPHIC SURVEYING

PREPARED BY

NORTECH SURVEYS (CANADA) INC.
319 - 2ND AVE S.W.
CALGARY, ALBERTA
T2P OC5

Tel: 403-262-0800
Fax: 403-262-0810

PREPARED FOR

CANADIAN HYDROGRAPHIC SERVICE
DEPARTMENT OF FISHERIES AND OCEANS
DSS CONTRACT SERIAL NUMBER FP802-7-2686/01SS

SCIENTIFIC AUTHORITY: MR. M. CASEY

APRIL 11, 1989

Table of Contents

1. INTRODUCTION.....1

2. CONTRACT RELATED DEVELOPMENT.....2
   2.1. HYDROSTAR Program Enhancements.....2
        2.1.1. General Hydrostar Development 2
        2.1.2. Norstar 1000 Decoding and Real Time Interfaci..3
        2.1.3. RTCM Differential Correction Format Developme..4
        2.1.4. Implementation of The RTCM Differential Corre..4
   2.2. Overview Of Multipath Analysis Techniques.....6
        2.2.1. Pseudo Range And Phase Smoothed Range Compari..6
        2.2.2. Signal Strength Variation Analysis.....8
        2.2.3. Fourier Transform Methods.....9
        2.2.4. Multipath Analysis Using GPS Phase Data.....14
   2.3. Pseudo Range and Carrier Phase Integration.....15
   2.4. Range Bias Feed Back.....19
   2.5. Proposal For Roll, Pitch and Heave Determination Us..20

3. GPS FIELD EXPERIMENTS.....21
   3.1. Oscillating Mast Experiment.....21
        3.1.1. Oscillating Mast Refurbishing.....21
        3.1.2. Angular Position Reference Program Developme..22
        3.1.3. Oscillating Mast Experiment Data Collection ..22
   3.2. RF Absorbent Ground Plane Experiment.....27

4. ANALYSIS OF RESULTS.....29
   4.1. Oscillating Mast Experiment.....29
        4.1.1. Establishment of Reference Positions.....29
        4.1.2. Multipath Analysis.....31
               4.1.2.1. Phase Smoothed and Pseudo Range Dif..31
               4.1.2.2. Signal Strength Variations.....37
               4.1.2.3. Fourier Analysis.....39
        4.1.3. GPS Positioning Results.....46
               4.1.3.1. Static GPS Positioning Results.....46
               4.1.3.2. Kinematic GPS Positioning Results....50
   4.2. RF Absorbent Ground Plane Experiment Results.....59

5. CONCLUSIONS AND RECOMMENDATIONS.....63

6. REFERENCES.....66

External Appendices

A. HYDROSTAR PROGRAM DEVELOPMENT.....1
B. NORSTAR 1000 BINARY OUTPUT DOCUMENTATION.....41
C. RTCM GPS DIFFERENTIAL CORRECTION STANDARD INFORMATION.....54
D. PROPOSAL FOR ROLL, PITCH AND HEAVE DETERMINATION USING ..71
E. MAST EXPERIMENT DATA.....80
F. RF ABSORBENT GROUND PLANE EXPERIMENT DATA.....158
G. MAST EXPERIMENT PHOTOGRAPHS 178
H. SYMPOSIUM PAPERS.....185

List of Figures

1. C/A Code Static High Multipath Pseudo Range Time Series G..7
2. C/A Code Static High Multipath Pseudo Range Histogram Gra..7
3. Phase Smoothed- Pseudo Range Difference Graph With Low Elevation Satellite.....8
4. Land Vehicle Kinematic Signal Strength Variations with Different Tracking Bandwidths.....9
5. MCAD Simulated Example Of FFT Filtering Using 64 Data Po..12
6. MCAD Simulated Example Of FFT Filtering Using 1024 Data ..13
7. Illustration Of Parallel Filter's Smoothed Range Misclos..17
8. Differential Corrections Day 223 Without Parallel Filter..18
9. Differential Corrections Day 223 With Parallel Filter 19
10. Quartz Quadratic Clock Fit Misclosures vs Time 20
11. Oscillating Mast Experiment Site Plan.....24
12. Polar Visibility Plot Day 218, 1988 U of C 32
13. Day 223 Oscillating Mast Kinematic Raw Pseudo Range Minus Phase Smoothed Range Variations.....33
14. Monitor Station Day 219 P Code Multipath 33
15. Monitor Station Day 223 C/A Code Multipath 34
16. Monitor Station Day 221 P Code Multipath 34
17. Pillar and Red Box Multipath P Code Example Day 221.....36
18. Pillar Multipath C/A Code Example Day 223.....37
19. Mast Experiment P Code Monitor Station Signal Strength Variation Graph Day 221.....38
20. Mast Experiment C/A Code Monitor Station Signal Strength Variation Graph Day 223.....38
21. Mast Experiment C/A Code Mast Station Signal Strength Variation Graph Day 223.....39
22. MCAD Multipath C/A Code Frequency Spectra Monitor Station Day 223 Prn 9 Start Time 18:30.....40
23. MCAD Multipath C/A Code Frequency Spectra Monitor Station Day 224 Prn 9 Start Time 18:26.....41
24. MCAD Multipath C/A Code Filtered Correlations Day 223/224 Monitor Station Prn 9.....41
25. MCAD C/A Code Frequency Spectra Kinematic Mast Day 223 Prn 9 21:05.....42
26. MCAD Multipath P Code Filtered Correlations Day 220/221 Pillar Station With Reflectors.....43
27. MCAD Multipath P Code Filtered Correlations Day 220/221 Red Box Station With Reflectors.....43
28. MCAD Multipath C/A Code Frequency Spectra Day 222 Pillar Station Without Reflectors.....44
29. MCAD Multipath C/A Code Frequency Spectra Day 223 Pillar Station Without Reflectors.....45
30. MCAD Multipath C/A Code Filtered Correlations Day 222/223 Pillar Station Without Reflectors.....45
31. NS1000 Static C/A Code Multi-Filter Position Deviation Graph Pillar Day 221.....46
32. NS1000 Monitor Station Multi-Filter Differential Correction Graph Day 221.....47
33. DRP 100% Phase Position Deviation Plot For Pillar Day 221.....48
34. DRP 100% phase Position Deviation Plot For Pillar Day 223.....48
35. DRP 100 % Phase Differential Corrections For

Monitor Day 221.....49
36. DRP 100 % Phase Differential Corrections
For Monitor Day 223 49
37. Day 221 P Code Kinematic Multi-Filter Position Graph.....50
38. Day 224 Multi-Filter Kinematic Position Graph.....51
39. Day 224 Multi-Filter Differential Correction Graph.....52
40. Day 223 Multi-Filter Kinematic Position Graph.....53
41. APR Minus GPS Position Difference Graph 100% Phase Day 2..55
42. APR Minus GPS Position Difference Graph
100% Phase Day 224, 1988.....55
43. APR Minus GPS Position Difference Graph
100% Phase Day 221, 1988.....56
44. APR Angle Derived Mast Velocity and Accelerations
Day 223.....57
45. APR Angle Derived Mast Velocity and Accelerations
Day 221.....58
46. APR Angle Derived Mast Velocity and Accelerations
Day 224.....58
47. P Code Pseudorange Noise Graph Without Absorbent
Ground Plane Day 312 14:00 - 15:00.....59
48. P Code Pseudorange Noise Graph With Absorbent
Ground Plane Day 311 14:00 - 15:00.....60
49. C/A Code Pseudorange Noise Graph Without Absorbent
Ground Plane Day 313 14:00 - 15:00.....60
50. C/A Code Pseudorange Noise Graph With Absorbent
Ground Plane Day 313 15:00 - 16:00.....61
51. C/A Code Pseudorange Noise Graph With Absorbent
Ground Plane Day 312 16:00 - 18:00.....62

List of Tables

1. Satellite Observing Schedule For Day 218 Aug 5 1988.....23
2. Mast Experiment TI4100 GPS Data Collection Summary.....26
3. Mast Experiment NS1000 GPS Data Collection Summary.....27
4. RF Absorbent Ground Experiment TI4100 GPS Data Collectio..28
5. U of C Monitor Station NOVAS Triangular Closure Summary...29
6. U of C Mast Test Station Final Coordinate Summary.....31
7. Summary Of Mast Experiment Pseudo range noise levels.....35

1. INTRODUCTION

This report reviews all work done under the contract entitled , **GPS at Sea For Hydrographic Surveying**, from Feb 29, 1988 to January 31, 1989. This contract was divided into three major tasks: HYDROSTAR GPS program enhancements, GPS positioning algorithm development, and the multipath field tests and related analysis. The first task was largely completed during the first five months of the contract and involved some general program development and enhancements. This was followed by the addition of Norstar 1000 GPS receiver data decoding support and RTCM differential correction standard software development (Section 2.1).

The second phase of contract work involved GPS positioning algorithm enhancements and the development of various multipath analysis methodologies. Multi-filter pseudo range and carrier phase measurement integration, range bias feedback, and roll, pitch and heave determination were the major areas covered (Sections 2.3-2.4). Four multipath analysis techniques were also developed and tested using previously collected data (Section 2.2).

A multipath test using an oscillating mast assembly to simulate a ship at sea was conducted at the University of Calgary in August (Section 3.1). This was followed by an absorbent ground plane multipath test in November which was also conducted at the U of C (Section 3.2). The analysis of these results, using the various methodologies developed, was conducted during the remainder of the contract.

The basic objectives of this contract were to: (1) upgrade the existing HYDROSTAR GPS positioning program, (2) develop improved positioning algorithms which exploit the use of accurate carrier phase measurements, and (3) determine the effects of antenna imaging and multipath on GPS measurements in a controlled kinematic environment.

During this contract the preparation of two technical papers (cf. Appendix H) was also accomplished. Supporting documentation for the program development, details of the GPS experiment data processing and analysis, and a set of experiment photographs are also contained in the various Appendices.

2. CONTRACT RELATED DEVELOPMENT

2.1. HYDROSTAR Program Enhancements

The initial work on this contract involved HYDROSTAR program development. This work was done on the Hewlett Packard 200 series (HP200) computer using the PASCAL programming language. The following sections outline the development accomplished in three distinct categories: general upgrades, Norstar 1000 (NS1000) GPS receiver data integration, and RTCM differential correction standard programming. A complete set of the revised HYDROSTAR user interface control screens and other relevant modification information are contained in Appendix A.

2.1.1. General Hydrostar Development

A worldwide WGS-84 geoid undulation table was added to HYDROSTAR in March. The source of this undulation table was the Ohio State University and it is identical to the one used by the NS1000 receiver with a resolution of one degree by one degree. Program development included: the addition of packed 97K binary lookup file, four point interpolation and other support subroutines, and associated user interface modifications and additions. The manual entry of single point and four point geoid undulations are also supported to incorporate more accurate localized information, if available.

Addition of various datum constants required for support of a rigorous 7 parameter transformation from the newly defined WGS-84 to various other datums was completed in April, 1988. This development work involved to a large extent the cleaning up and augmentation of existing code with only minor revisions and extensive testing. The HYDROSTAR program now supports conversion from the GPS WGS-84 datum to the NAD-83, NAD-27, and WGS-72 datums or any "users defined" datum.

The expansion of graphics and waypoint navigation algorithms to support UTM in addition to geographic coordinates was also completed and tested. This involved the writing of several new subroutines and extensive user interface modifications on the navigation/waypoint and graphics control screens. Other miscellaneous enhancements to the program included: multi-unit velocity display, post processing data decimation options, and hard copy output of program initialization data. The incorporation of an automatic or manual heading entry for kinematic offset position calculation was also added.

The HYDROSTAR program's external interface capabilities were augmented with the addition of two serial output ports. This involved significant control screen modifications and the addition of several low level support subroutines to enable the setting of the serial port attributes. The optional serial interface attributes incorporated were baud rate (300 to 19.2K), parity, and the number of data and stop bits. The ASCII data logger routines

and control screen were also modified to support an additional output port. This was done to enable a dedicated output for a second logging device such as an ISAH data management system. The serial output development was primarily done to support the ISAH system and enable RTCM output suitable for radio modem transmission. Another benefit of this development was the support for input of GPS data from receivers with different serial output specifications (cf. Section 2.1.2).

After discussions with Questor Tangent, an ISAH position data format for both the HYDROSTAR program and the Norstar 1000 receiver were formulated. This information was implemented, documented, and sent to Questor Tangent for inclusion in the ISAH system. Subsequent discussions with the CHS resulted in the addition of a heave value to the HYDROSTAR output to support future development in this area. A successful bench test was conducted in Calgary in early June using the actual hardware components. Minor modifications to ISAH internal software were made at this time and tested to ensure proper data decoding. After this test, finalized HYDROSTAR and Norstar ASCII output documentation was forwarded to Questor Tangent for inclusion in their final report for CHS (cf. Appendix A).

2.1.2. Norstar 1000 Decoding and Real Time Interfacing

This development was initiated in early March and successfully completed and tested. PASCAL subroutines were written to decode all NS1000 binary output including almanac, ephemeris, and raw pseudo range and phase measurement data. These program additions were accompanied by appropriate channel dimension changes to support 5 instead of 4 observed satellites. The complete NS1000 binary data output specifications are contained in Appendix B.

The re-dimensioning from 4 to 5 satellites affected several other areas of the HYDROSTAR program including those for data base input, navigation filter computations, screen display, and ASCII data logger output. Fortunately the HYDROSTAR data base was originally designed to be compatible with the NS1000 receiver so most of the modifications were minor. The real time data interface was also tested with a NS1000 receiver and the effective computation rate of 2 seconds was achieved. Serial port configuration routines were tested at this time to ensure their correct operation using various input data rates (including 19200 baud) and other attribute settings.

Currently the HYDROSTAR program can support both the 4 channel TI4100 raw binary output and 5 channel NS1000 1Hz and 5Hz binary data output structures. Possible future developments in this area include expansion of the HYDROSTAR program to support 7 channel NS1000 data and additional decoding capability for another GPS receiver, which has not yet been specified by the CHS. Unfortunately the NS1000 binary data output structures were

modified when the internal receiver software was upgraded for seven channels (Dec 14, 1988) and the HYDROSTAR program will require some minor revisions.

2.1.3. RTCM Differential Correction Format Development

The development of a suitable data format standard for the real time transmission of GPS differential corrections was a task undertaken by RTCM (Radio Technical Commission for Maritime services, Washington, D.C.) special committee SC-104. It was decided by CHS to develop the software to support this standard so that shore based transmission of GPS differential corrections, using a radio link with a low data rate (e.g. 50 bits per second), could be realized.

Using the March 1, 1988 version of the RTCM standard, the software required to encode and decode the various differential correction message types was developed on the HP200 series computer in PASCAL. This software was tested using two computers, a serial data link, and simulated data. Verification of the message content and the testing of various subroutines required for frame synchronization, parity formulation, and error detection and correction was accomplished during this phase of the development.

Since this contract was started (Feb 29, 1988), many organizations and groups using the RTCM standard have conducted numerous field trials and given their recommendations for revisions to the SC-104 group (cf. Appendix C). The RTCM software development was abandoned, prior to full implementation within the HYDROSTAR program, after it was learned in August 1988 that numerous changes were planned for the message content and format. The final RTCM release date is tentatively scheduled for early 1989 (personal communication with R. Kalufus) and a partial draft copy is included in Appendix C.

2.1.4. Implementation of The RTCM Differential Correction Format

A disadvantage of using the RTCM standard for transmission of differential corrections is that it has a general design with a certain amount of computational and other overhead which is not necessarily required for specific hydrographic surveying applications. Advantages of using the RTCM standard for transmission of differential corrections are as follows:

1. The RTCM standard has been designed and updated by the user community to ensure adequate testing and incorporation of several desirable features including special high rate messages to counteract control segment SA measures, high accuracy survey type information including carrier phase measurements, and status and health messages to help ensure system integrity and improve system performance.

2. It will probably be adopted by GPS receiver manufacturer's meaning the internal processor of the receiver will handle the required computational tasks for encoding and decoding of the RTCM message with the user responsible for the communications interface (e.g. radio modems).

3. Government and private services will likely use the standard and transmit RTCM GPS information using existing radio beacons and other coastal systems in areas where it economically feasible. Certain message types have also been reserved for the Coast Guard to transmit differential Loran-C and Omega data, weather messages, and Notices To Mariners.

4. Pseudolite transmission information and timing capability are supported within the RTCM standard due to its use of the GPS standard word length, 50 bps data rate, and parity algorithm for error detection.

5. A users equipment interface using full duplex serial standards is specified meaning that two way communications between the reference station and the user are possible. Additionally a system may be configured using existing hardware instead of more expensive specially designed components.

It was decided at the October CHS GPS working group meetings to re-evaluate the final RTCM standard in the future and access its merits in view of specific CHS requirements. There is also some uncertainty regarding the effectiveness of this standard in view of the implementation of SA (Selective Availability) measures by the GPS MCS (Master Control Segment). Current information regarding SA measures indicate they will be be done using two methods. The first, referred to as Epsilon, involves errors introduced into the transmitted GPS navigation message. The second involves dither of the satellite reference oscillator to degrade phase and pseudo range measurement accuracy. It should be possible to access SA effects on GPS differential corrections when the first Block II satellite, (launched February 14, 1989) is operational.

2.2. Overview Of Multipath Analysis Techniques

To assess the effects of both GPS pseudo range and phase measurement multipath effects under this contract, many methods were used. The previously developed methods of pseudo range and phase smoothed range comparison and signal strength variations are first reviewed. This is followed by development of two new methods involving the use of Fourier transforms and phase derived position comparisons. Results derived from experimental data collected under this contract are analyzed in section 4 with additional data graphs and statistical tables contained in Appendix E.

2.2.1. Pseudo Range And Phase Smoothed Range Comparisons

This method of pseudo range multipath determination involves the comparison of raw GPS pseudo ranges with corresponding phase smoothed ranges provided by the pseudo range and phase integration filter (cf. Section 2.3). The time required for filter stabilization varies depending on the variances of the contributing elements and generally takes place within the first 200 observations or about 4 minutes assuming a raw measurement data rate of 1 second. The contribution of pseudo range errors to the phase smoothed range after filter stabilization is effectively negligible due to the relative magnitudes of the measurement errors. This technique provides useful information on pseudo range noise levels (Figure 1) and the normality of range errors (Figure 2). It also allows the magnitude and period of multipath induced pseudo range errors to be quantified by day to day correlations of GPS data collected from the same static observing sites (cf. Tranquilla, 1988).

This method of multipath analysis is not without problems. The first problem is that a certain amount of data is required for phase smoothed range stabilization. This initial period is influenced by the noise levels present in the raw pseudo ranges, the receiver data output rates, the smoothing function phase weighting curve (controlled by the variances of the contributing components) and the upper phase weight limit used in generation of the differences. Another related problem arises when analyzing low elevation satellites using single frequency data due to the use of modeled ionospheric phase advance to map phase measurements onto pseudo ranges. A significant divergence occurs when using high phase weighting in combination with low elevation satellites which results in the biasing of the difference statistics. An example of this is illustrated in Figure 3 with satellite prn 6 where the elevation is decreasing from 35 to 20 degrees over the time period from 20:00 to 20:30 hours.

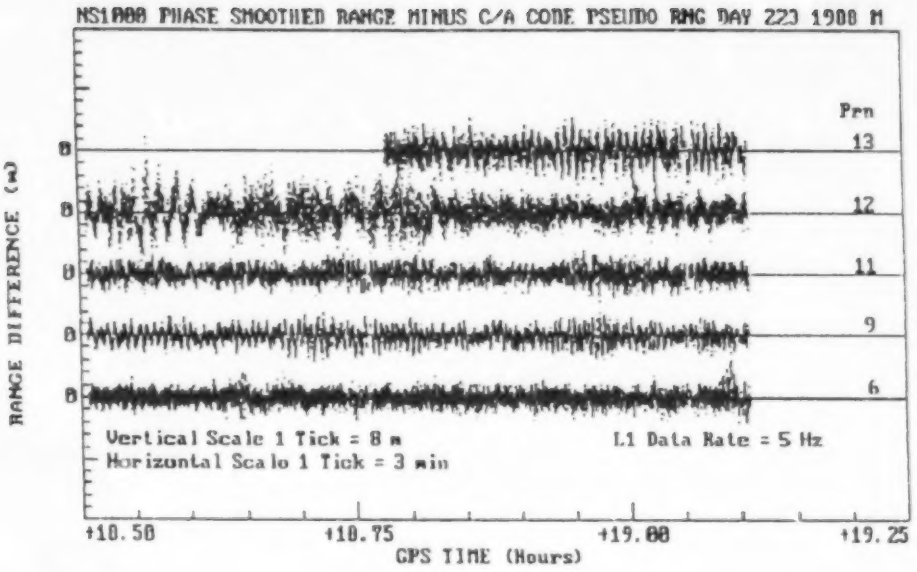

Figure 1. C/A Code Static High Multipath Pseudo Range Time Series Graph

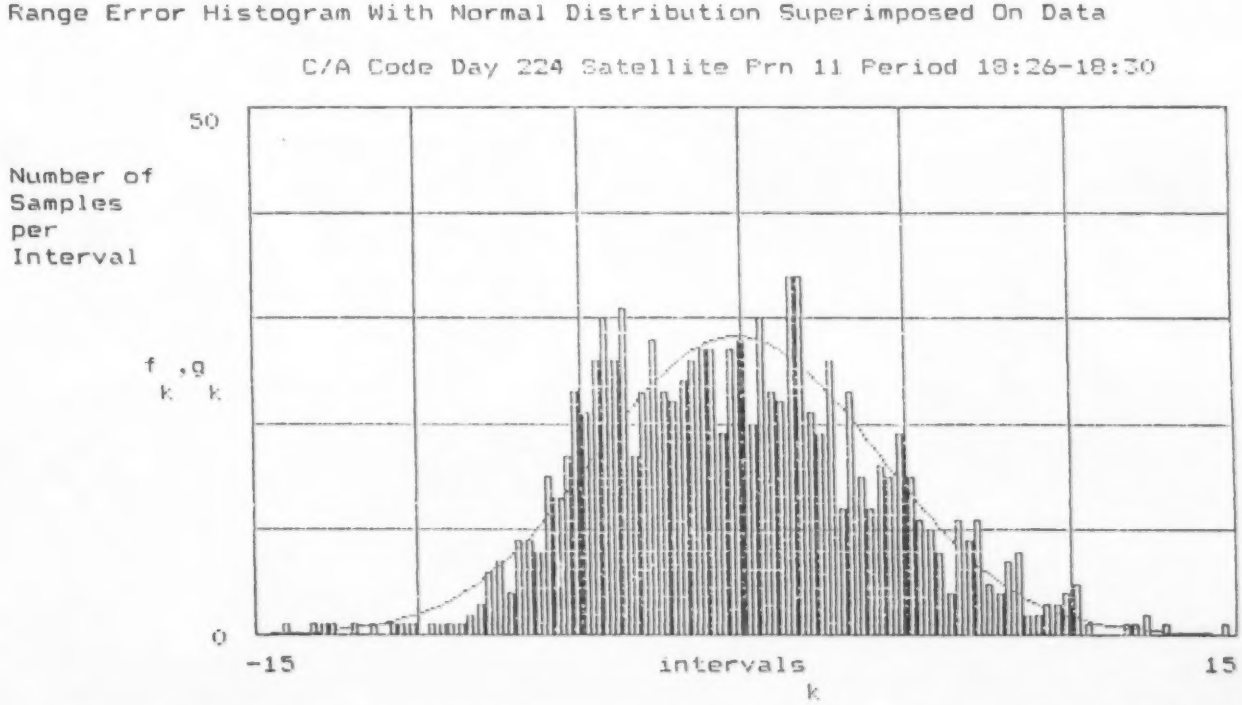

Figure 2. C/A Code Static High Multipath Pseudo Range Histogram Graph

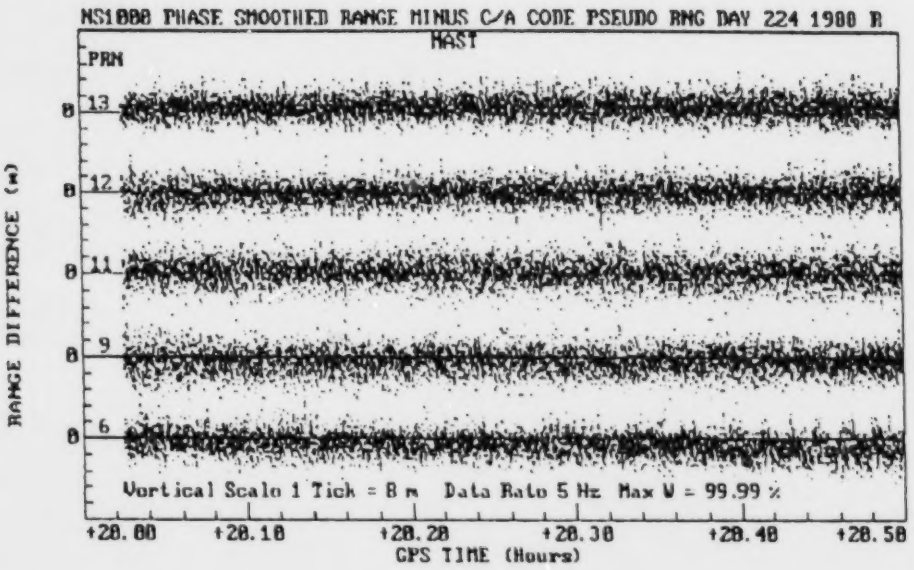

Figure 3. Phase Smoothed- Pseudo Range Difference Graph With Low Elevation Satellite

Another deficiency in the method of phase and pseudo range differences is in the implicit assumption that the phase measurements are unaffected by multipath. The fact is that there are random and systematic variations in phase measurements due to tracking bandwidth, ionospheric noise, site related multipath, antenna phase center variations, and antenna imaging effects. The magnitude of these variations is, however, much less than code noise levels and would be worth isolating only in the determination of medium to long period multipath on P code data. With C/A code data, the noise levels are sufficiently different in magnitude that phase errors have little if any effect in the final results. More information regarding the variations of phase measurements due to multipath is presented in sections 2.2.4 and 4.1.2.

2.2.2. Signal Strength Variation Analysis

Another method useful in the analysis of multipath phenomena involves the use of receiver signal strength data. It is easily verified that significant code multipath variations are accompanied by corresponding fluctuations in signal strength. Although the determination of magnitude and periods of multipath using this method are not as effective as the previous method of range comparisons, there are some useful insights provided using this method.

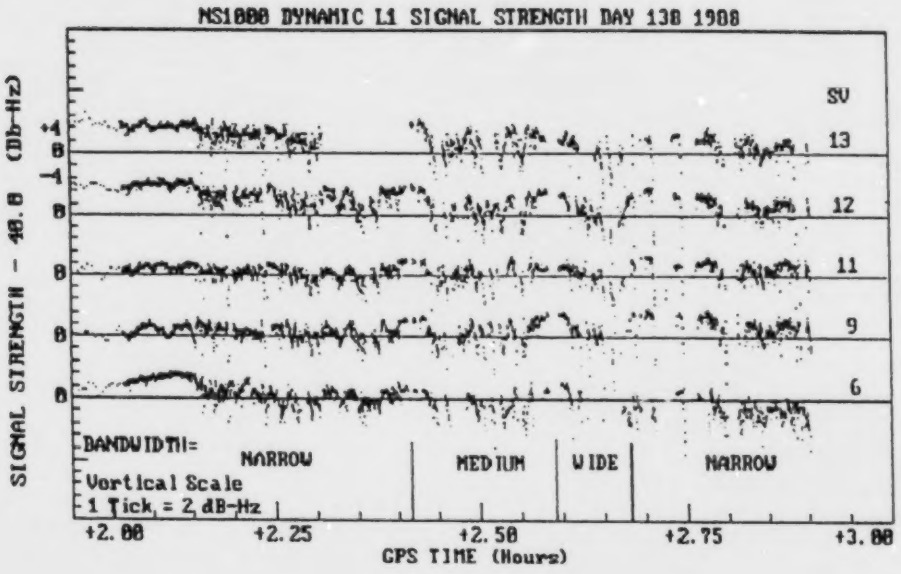

Figure 4. Land Vehicle Kinematic Signal Strength Variations with Different Tracking Bandwidths

The verification of other multipath determination techniques and the comparison of signal strengths using different receiver tracking bandwidths under both static and kinematic conditions is possible. An example of the this is illustrated in Figure 4. There is a distinct difference between static (from 2.0 to 2.15 hours) and kinematic signal strength variations and noticeable degradation at the wider bandwidth settings as expected. More data analysis using this technique are presented in section 4.1.2 and Appendix E.

2.2.3. Fourier Transform Methods

This section introduces the technique of using the FFT (Fast Fourier Transform) on GPS pseudo range data to filter high frequency noise and accurately quantify multipath phenomena. The physical basis for this method arises due to the fact that periods of pseudo range multipath, caused by reflective objects in the vicinity of the GPS receiving antenna, will be of relatively long duration due to the slow variation in position of the transmitting satellite with respect to the observer and the reflector. Following a brief overview of the basics of Fourier transforms, some illustrative examples using simulated data are presented.

The Fourier transform of a periodic time domain function results in a frequency domain representation of the function composed of a finite number of sinusoids of different amplitude and frequency [Brigham, 1974]. In exponential form this transform is represented by the Fourier integral i.e.:

$$H(f) = \int_{-\infty}^{\infty} h(t)\exp(-i2\pi ft)\, dt \qquad (2.1)$$

where:

h(t) is a function defined in the time domain,

H(f) is the transform function defined in the frequency domain, and

i = the imaginary unit ($\sqrt{-1}$).

The solution to equation 2.1 for a continuous function, if it exists, will yield a continuous spectral representation of the original function. For a periodic time domain function sampled with n equally spaced values, the frequency domain representation may be determined using the discrete Fourier transform. The FFT is just a computationally efficient algorithm of determining the solution of a discrete Fourier transform. More specifically instead of n^2 operations, the FFT requires only $n \cdot \log_2 n$ operations [Blais, 1987].

The IBM PC based MathCAD (MCAD) program, developed by MATHSoft Inc., was used for the FFT analysis of GPS pseudo range data. The discrete fast Fourier transform (fft(v)) formulation used by MCAD is given as:

$$c_j = (1/\sqrt{n}) \cdot \Sigma_k \, v_k \exp\,(2\pi i \cdot (j/n) \cdot k) \qquad (2.2)$$

where:

v = vector of n real equally spaced measurements in the time domain data,

n = the number of samples in v and must be an integer power of 2 (i.e. 2^m),

c = vector of j complex coefficients representing values in the frequency domain and contains $2^{m-1}+1$ values, and

i = the imaginary unit ($\sqrt{-1}$).

The discrete inverse fast Fourier transform (ifft(v)) used by MathCAD is given as:

$$d_j = (1/\sqrt{n}) \cdot \Sigma_k \, w_k \exp\,(-2\pi i \cdot (j/n) \cdot k) \qquad (2.3)$$

where:

v = vector of 2^m+1 real frequency domain samples similar to c in the preceding formula,

w = vector composed of v with the conjugates of v appended, and

d = resultant vector of n complex coefficients representing values in the time domain where $n = 2^{m+1}$.

The FFT method has limitations in terms of frequency resolution and problems with spectral leakage often arise. The limit of frequency resolution is the reciprocal of the length of the observation record. Leakage results when the energy of the predominate frequencies leaks into the other frequency components resulting in distortions or in some cases complete masking [Blais, 1987]. Another problem is aliasing or distortions in the frequency spectra which are caused when the sampling interval is not large enough. To avoid this the Nyquist sampling rate, defined as the interval of twice the period of the desired signal (i.e. T = 1/(2f)), must be used [Brigham, 1974]. There are also practical FFT limitations which arise from the fact that the number of data points must be an even power of two and zero padding or truncation of the time series may result in distortions of the spectral components.

Some of the FFT limitations are illustrated by the following examples which make use of a simulated data sequence (borrowed from Blais, 1987) which consists of three distinct frequencies of two different amplitudes. In the first MCAD example (Figure 5) a short sequence of 64 data points is used. The resulting spectral leakage is evident in the frequency spectrum graph which seems to have only one predominant frequency instead of three with two close together as indicated by the data generation function.

In the next set of graphs (Figure 6) the number of data points has been expanded to 1024 points and the three frequency components are clearly visible. Even with a large amount of noise added to the original data, the effectiveness of this method of filtering with larger sample sizes is illustrated by the similarity of the original and final time series data graphs. There is however a small error in the spectral amplitude of the second frequency component since it is not identical to the third.

FILTERING A NOISY SIGNAL WITH FFT π = 3.14159

Define the signal: i := 0 ..63

$q_i := \cos(0.2 \cdot \pi \cdot i) + 3.1622 \cdot \cos(0.4 \cdot \pi \cdot i) + 3.1622 \cdot \cos(0.42 \cdot \pi \cdot i)$

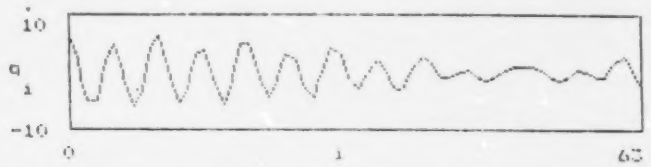

Add some noise:

$s_i := q_i + (rnd(2) - 1.0) \cdot 5.0$

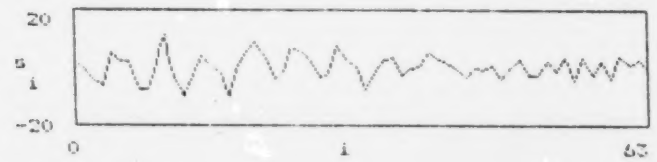

Take its discrete fourier transform:

f := fft(s) j := 0 ..32

α := 7.0 ...define threshold for spectral noise rejection.

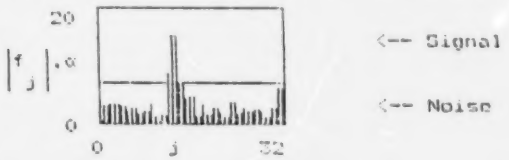

Filter, and take the inverse transform:

$g_j := f_j \cdot \mathbb{I}\left[\left|f_j\right| - \alpha\right]$ h := ifft(g)

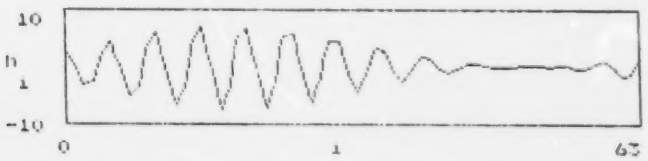

Figure 5. MCAD Simulated Example Of FFT Filtering Using 64 Data Points

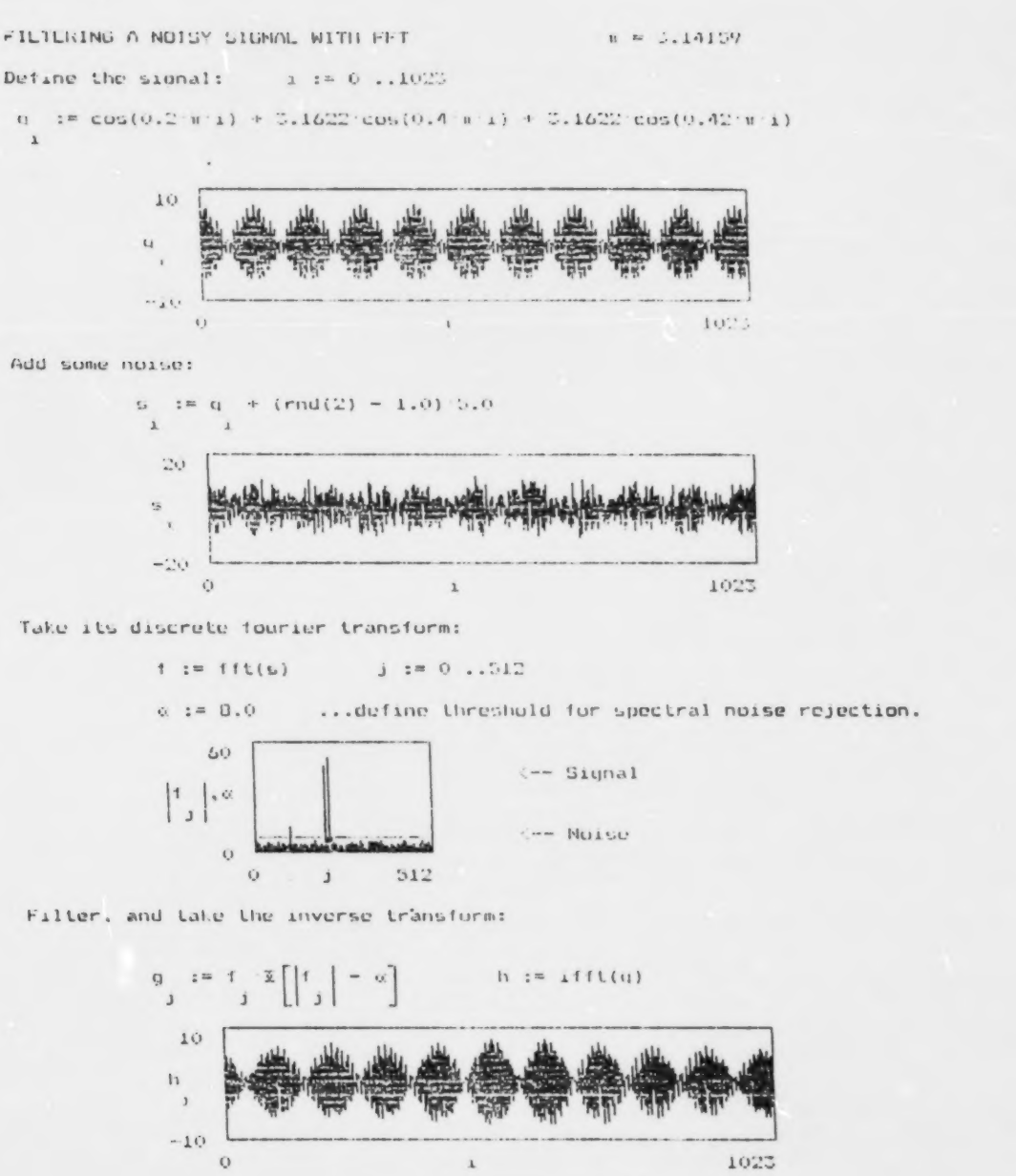

Figure 6. MCAD Simulated Example Of FFT Filtering Using 1024 Data Points

The pseudo range and phase smoothed range difference data discussed in Section 2.2.1 were used for MCAD FFT analysis to help identify multipath effects on high noise C/A code pseudo data. Day to day time shifted data was used to analyze the correlation of multipath phenomena for the various stationary an-

tenna locations used in this experiment. The MCAD processing results are discussed in Section 4.1.2 with the complete supporting output examples contained in Appendix E.

2.2.4. Multipath Analysis Using GPS Phase Data

The final method of analysis, which provides a way of determining phase measurement multipath, involves the use GPS phase data from known positions in conjunction with a modified positioning algorithm. This technique, referred to as the discrete relative phase (DRP) method, is different from previous methods in that it is independent of pseudo range data and requires apriori knowledge of antenna positions. It differs from static double difference phase methods (e.g. NOVAS) in that it is applicable to situations where the remote is non-stationary.

Basically the DRP method functions as follows:

1. The known position of the monitor is used to form a theoretical range to the satellite which is substituted for the measured pseudo range at the first epoch.

2. For each epoch following this, the change in range derived from phase only is used in conjunction with the previous epochs range, to form a new range.

3. With a set of these ranges, an adjustment is performed to remove local clock offset and the resulting range residuals, corresponding to the monitor station's fixed location, are used to form differential corrections for the current epoch.

4. Using these phase derived differential corrections, a remote station's data is then processed similar to steps 1 and 2, however the position is unconstrained in the adjustment stage (step 3).

Since the theoretical position is used to derive the initial ranges and the differential corrections are zero at the initial epoch, the remote station's starting position will be the same as known reference position. The monitor station must be stationary while the remote must have a precisely known starting location. Any errors in these positions will result in systematic growth of positioning errors as the geometry of the observing satellites changes over time. This method also breaks down with increasing baseline separation due to atmospheric error de-correlation and must be used with cycle slip free phase data.

Any phase measurement errors due to antenna phase center variation (caused by design deficiencies or local imaging effects), reflective surface induced multipath , or dissimilar receiver measurement characteristics (e.g. due to different bandwidth settings), will result in variations in the remote station's position. If the identical receivers are used with similar antennas and phase measurement errors, it is reasonable to assume the remaining errors will be, for the most part, due to

differences in their local receiving environment. It follows then that large variations in positions which correlate to similar large variations in the differential corrections may be attributable to monitor station phase measurement multipath errors. Conversely remote position variations, not attributable to monitor station differential correction errors, must be due to locally induced phase multipath. This premise can be verified by time shifted correlations of two or more days of data collected from the same station as described in Section 2.2.1.

The DRP method was used for data analysis for the oscillating mast experiment (described in Section 3), since the reference locations were known very accurately (cf. Section 4.1.1) and the short baseline separation (25 m) minimized the effects of atmospheric de-correlation errors. Both static and kinematic data sets were used for the multipath analysis and very good positioning accuracies were obtained.(cf. Sections 4.1.2 and 4.1.3).

2.3. Pseudo Range and Carrier Phase Integration

The real time combination of GPS pseudo range and phase measurements results in a significant increase in differential positioning accuracy. The improvement of accuracy is however limited by the random and systematic errors present in the pseudo range measurements (e.g. multipath) and the frequency of cycle slips in the phase measurements. The degradation in positioning accuracy is further influenced by uncorrelated errors (e.g. due to the atmospheric effects) between the stationary monitor and dynamic remote receivers. The technique of range and phase integration and its associated error sources has been fully documented in a previous report (cf. Nortech, 1987) and will not be repeated here.

A major objective of this contract was to improve the pseudo range and phase integration method to provide more accurate final positions. This was accomplished by the development of a multi-filter integration method which basically monitors the performance of a main filter with two offset parallel filters. If large pseudo range multipath errors have resulted in the biasing of the main filter, a partial reset using the alternate filter's data is possible. This technique allows a higher weight to be used on the phase without undesirable biasing errors which systematically increase over time.

A major assumption regarding this method is that pseudo range errors are for the most part random and normally distributed in time. In the presence of multipath, phase measurements are not significantly affected and the periods of large pseudo range systematic errors are of relatively short duration (i.e. from 10-30 seconds up to few minutes, cf. Figures 1 and 11). Other systematic errors, arising from using a modeled ionospheric phase advance to correct the phase measurements, are adequately reduced at higher elevations by not over weighting the phase measurements (i.e. a limit on phase weighting of 99.97 % is appropriate for most applications). At lower elevations, addi-

tional de-weighting of the phase measurements is required to avoid divergence between the phase smoothed and raw pseudo ranges.

The use of a higher phase weighting scheme to reduce pseudo range multipath errors present in the phase smoothed ranges is possible but can result in other problems. Adequate counter measures to detect the biases that may occur during filter stabilization must be in place. In the case of C/A code receivers, pseudo range multipath errors can easily reach 10 metres and the dissipation of a large initial bias can take take as long as 15 minutes, depending on the phase weight limit and measurement data rate. By specifying the limit on parallel filter reset, to a time greater than the period of multipath, and setting the test limit for a filter reset above the residual noise levels present in the phase smoothed ranges, effective measurement integration is accomplished.

A multi-filter algorithm was implemented and tested using the oscillating mast experiment data. Two parallel filters are run for each range using the standard phase phase weighting function (max limit 99.5%). The first one is started at the same time as the main filter and resets each time a maximum count, specified by the operator, has been reached. A second filter is started half the maximum interval after the first to give a 50 % overlap. When the maximum count has been accumulated by either filter, a test is made on the misclosure between the two phase smoothed ranges.

This misclosure is actually a smoothed value (cf. Figure 7) formed using a variance derived weighting function and the raw difference between the phased smoothed ranges from the main filter and the parallel filter i.e.:

$$dr1_i = smr1_i - smr0_i \tag{2.4}$$

$$dr1_var_i = smr1_var_i + smr0_var_i \tag{2.5}$$

$$rng_miscl_var1_i = rng_miscl_var1_i + 0.10 \tag{2.6}$$

$$w1 = dr1_var_i \,/\, (rng_miscl_var1_i + dr1_var_i) \tag{2.7}$$

$$rng_miscl_var1_i = 1.0/((1.0/rng_miscl_var1_i) + (1.0/ dr1_var_i)) \tag{2.8}$$

$$rng_miscl_1_i = w1 * rng_miscl_1_i + (1.0 - w1) * dr1_var_i) \; ; \tag{2.9}$$

where:

$smr0_i$ = current main filter smoothed range,

$smr1_i$ = current filter 1 smoothed range,

$smr0_var_i$ = main filter smoothed range variance,

$smrl_var_i$ = filter 1 smoothed range variance,

$rng_miscl_1_i$ = smoothed filter 1 range misclosure,

$rng_miscl_varl_i$ = smoothed filter 1 range misclosure variance, and

i = channel index.

Both the filter smoothed range misclosure and its variance are carried from one epoch to the next and a process noise variance of 0.10 m^2 is added (equation 2.6) to ensure over weighting of previous data does not occur.

If an operator selectable limit (e.g. 2 metres) has been exceeded, a partial reset, which is done by an averaging of the parallel filter's data with the main filter, occurs. The phase weighting of the main filter is increased to a selectable limit (default 99.97 %) after it exceeds a preset limit of 99.5 %. It may however be reduced to a lower level, based on satellite elevation, by enabling an ionospheric phase advance variance option. In this case the threshold variance before modification is set to a lower test value of 99.0 %.

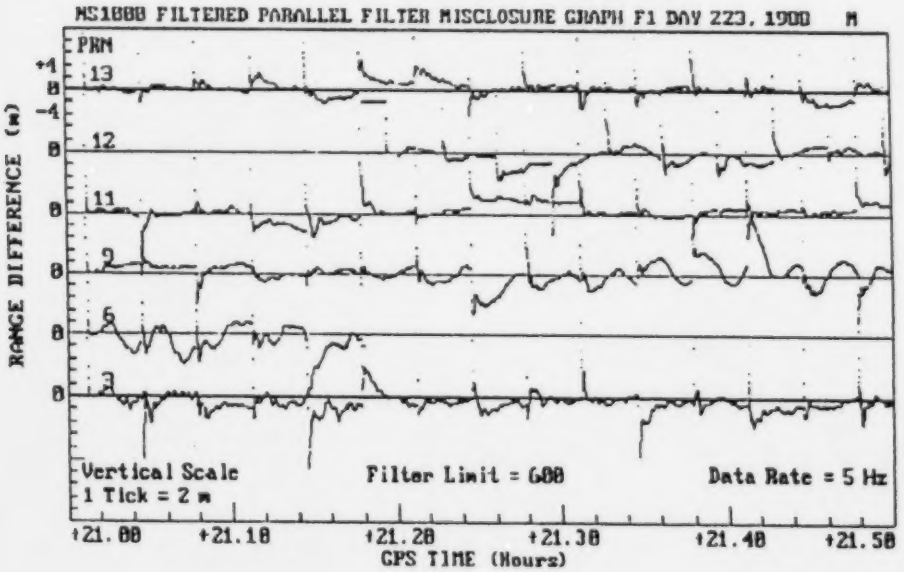

Figure 7. Illustration Of Parallel Filter's Smoothed Range Misclosures

To tune the filter for static station GPS data with severe multipath, knowledge regarding the duration and magnitude of the multipath is important. A special diagnostic display, which con-

tinuously monitors the misclosures between the main filter range and the two parallel filter ranges, is provided. If the parallel filter's period is too short, frequent resets to biased values will result. Conversely, a longer reset period, will result in prolonged main filter systematic errors. If a phase weight limit is too high, systematic trends in the phase smoothed range will result, particularly at lower elevations. If too low a phase weight is used, the residual noise left in the final ranges will seriously degrade positioning accuracies, especially during periods of poor SV geometry. If a cycle slip occurs or if after stabilization a prolonged large misclosure between the main filter's range (>35 m) and the raw pseudo range exists, both the main filter and the two parallel filters will be reset. The advantage of a parallel filter is best realized at a stationary monitor site with large multipath induced errors and an example of differential corrections generated both with and without this algorithm are shown in Figures 8 and 9.

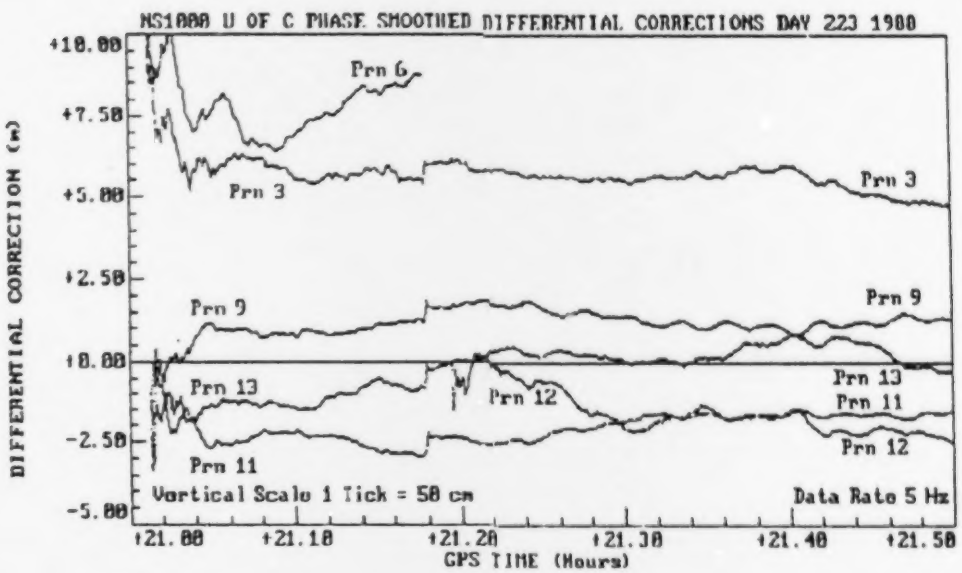

Figure 8. Differential Corrections Day 223 Without Parallel Filter

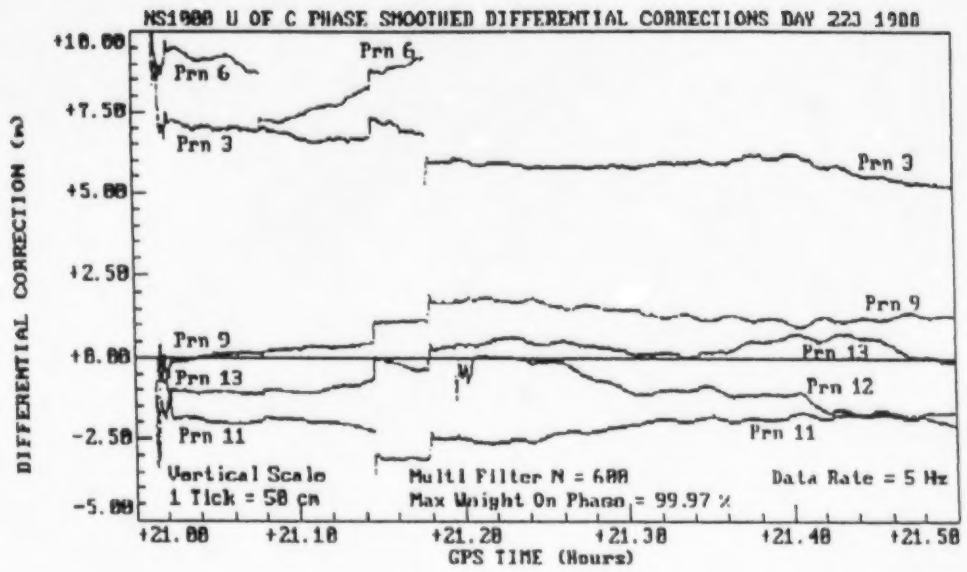

Figure 9. Differential Corrections Day 223 With Parallel Filter

2.4. Range Bias Feed Back

The HYDROSTAR program models the receiver local clock errors of the internal quartz oscillator using a three coefficient (quadratic) model to incorporate estimates of the offset (range bias), drift, and drift rate. A two coefficient linear model is used if an external cesium or rubidium frequency standard is controlling receiver time. To generate the coefficients, a least squares type estimator algorithm is used which basically operates as a fading memory filter complete with process noise tuning constants which are clock type specific.

The algorithm for range bias feedback is based on the assumption that if a reasonable knowledge of the users clock error is available, this information can be used to improve the positioning solution. The actual implementation is done with a test on the quality of the clock fit and is followed by a recalculation of the least squares position solution using the modeled clock value and its associated variance as an apriori parameter constraint. The first solution results in a updated clock fit while the second solution results in a slightly modified position with a corresponding reduction in height variance. This reduction in height variance is related to the high correlation between range bias and height through satellite geometry.

The value of the clock fit misclosures using phase smoothed pseudo ranges varies ±5 cm. (cf. Figure 10). The result of range bias feedback is a reduction in the limited high frequency noise of the height. Its absolute value from the positioning solution is only slightly modified. Both the HYDROSTAR clock fit and range bias feedback algorithms operate in real time and in post processing mode. It is evident from the small fit misclosures (Figure 10) that range bias feedback is of little benefit if a sufficient number of satellites are available.

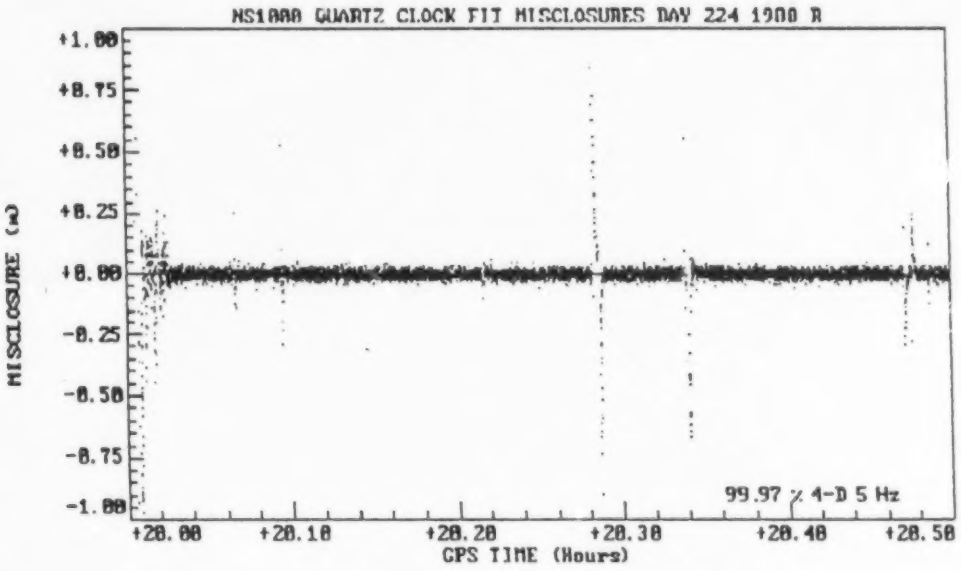

Figure 10. Quartz Quadratic Clock Fit Misclosures vs Time

2.5. Proposal For Roll, Pitch and Heave Determination Using GPS

The use of precise GPS phase measurements to aid in the correction of hydrographic sounding data through heave estimation of a vessel, was a topic of investigation covered under the current contract. Basically the fundamental question is: can relative GPS phase data be used to determine accurate ship height with respect to the the instantaneous sea level free from the effects of the waves which cause heave motion. Corrections are also required to account for the antenna's displacement due to roll and pitch of the vessel. The proposal included in Appendix D outlines three alternative methods for accomplishing this task: unaided GPS, GPS aided with low cost attitude sensors, and GPS aided with attitude sensors and a gyro compass or other direction sensor. Although it is not possible to assess these methods accurately at this time, it is proposed to conduct simulations and a shipborne test at a later date. Equipment would include a 5 Hz multi-channel GPS receiver, various direction sensors, and a low cost roll and pitch sensor.

3. GPS FIELD EXPERIMENTS

3.1. Oscillating Mast Experiment

To analyze the effects of pseudo range and phase measurement multipath on kinematic GPS positions, data was collected using an oscillating mast assembly on the roof of the engineering building at the University of Calgary. This experiment required significant preparation in the form of mast assembly refurbishing, angular position hardware and software development, and multipath inducement measures. The following sections overview the mast assembly development and the details of the experiment data collection performed during the first two weeks of August, 1988.

3.1.1. Oscillating Mast Refurbishing

The determination of the oscillating mast assembly antenna position was previously performed using an electrical sensing device mounted on the axle at the base of the drive mechanism (cf. NORTECH, 1986). This design had some problems, the first being in the provision of electrical closures from the main drive (i.e. spikes were prevalent in positions due to double closures). The second problem involved the generation of mast antenna positions. These positions were based on a theoretical linkage model which was only an approximation of the actual drive mechanism due to flexure in the various component parts.

To enhance the accuracy of the determination of mast angle, a re-design was initiated under this contract. This re-design involved the addition of an optical encoder connected directly to the rotation axis of the mast. This resulted in much more accurate determination of mast positions since deficiencies in the drive mechanism have no effect on precise angular determination. This new mast positioning technique also required the development of a microprocessor based unit, referred as the APR (Angular Position Reference), to accept the encoder output, form an angular value, and output it on a serial interface for monitoring and recording purposes. The APR unit also generates an electrical closure, at the precise instant in time for which the angular value applies, so a time tag can be associated with each angular measurement.

In late July the writing of the APR microprocessor program was completed and tested. Features of the APR unit include a reset switch for calibrating of the zero degree reading (i.e. when the mast is vertical) and a four position switch for the minimum change required for angular output (1, 2, 4, or 8 degrees). The required fabrication and machining for mounting of the angular encoding device was then done. The final phase of mast refurbishing involved mounting of the APR and optical encoding device and the installation of guy wires for additional tower support to reduce flexure.

The optical encoder generates 8192 counts per 360 degrees of rotation which gives it a minimum angular resolution of 2.6367 minutes of arc. With a gear ratio between the mast and the optical encoder of 256/360, the least significant bit (one encoder count) represents a mast angle of 1.875 minutes of arc. Assuming a mast length of 4.3 metres, the theoretical mast positioning accuracy is 2.345 mm. There are, however, physical sources of error between the optical encoder and the phase center of the GPS antenna on the mast which slightly degrade this positioning accuracy such as tower flexure and centering errors.

3.1.2. Angular Position Reference Program Development

The final stage of development before field data collection, involved the writing of a program on an HP220 computer to receive APR angle data, time tag it using output from the CAPTS (Computer Addressable Precision Timing System) clock, and record it for future analysis. This APR program was augmented to synchronize the CAPTS clock to GPS time using the serial data output of either the TI4100 or NS1000 GPS receivers for user clock offset correction and the 1 PPS (one pulse per second) output for a trigger.

The resolution of the APR latched time provided by the CAPTS clock is 0.1 msec. Since a rubidium frequency standard was used to control the CAPTS, the drift between the CAPTS time and GPS time over a 5 hour period was insignificant (1 part in 10^{-11}). Assuming a 30 degree swing angle, a mast length of 4.3 metres, and an oscillation period of 8 seconds, the maximum error in the time tagging of an APR angle would only introduce an error of 0.1 mm in the final mast GPS antenna position.

The real time APR program basically reads the APR latched time in the form of an ASCII string (HH:MM:SS.SSSS) from the CAPTS clock and a single byte representing the mast angle from the 9600 baud serial output of the APR on an interrupt basis. The latched time interrupt from the CAPTS is generated by the pulsed output from the APR as the minimum change in angle is sensed (e.g. every one degree). After reading this information, it is reformatted to a GPS time in seconds (from the beginning of the day) and an angular value in degrees. These two values were then written to a data tape using a buffered serial output. It was found after testing, that the highest angular output rate on the APR (one degree) could be used without any buffering problems. Therefore this setting was used for the entire experiment.

3.1.3. Oscillating Mast Experiment Data Collection

A sub-contract report by Jim Tranquilla was received May 7 which outlined procedures for performing multipath testing using reflective panels. These suggestions were reviewed and a test plan was formulated in late July. The observing periods and satellites to be tracked were then determined using a GPS alerts program to optimize the length of observing period for both a 4

and 5 satellite constellations and ensure acceptable 4-D GDOP (cf. Appendix E). The use of both stationary and dynamic remote antenna locations for GPS observations were incorporated in the experiment to enable better assessment of the effects of induced multipath on GPS pseudo range and phase observations.

Table 1. Satellite Observing Schedule For Day 218 Aug 5 1988

Period (min)	GMT Time	LOCAL Time	Best 4 Sv Prns	5	GDOP (4 sv)
1 (40)	18:50	12:50pm	6,9,11,12	13	6.8
	19:30	1:30			5.6
2 (50)	19:30	1:30	6,11,12,13	9	5.6
	20:20	2:20			5.1
3 (40)	20:20	2:20	6,9,12,13	11	5.1
	21:00	3:00			5.7
4 (30)	21:00	3:00	3,6,9,11	13	4.5
	21:30	3:30			3.7
5 (60)	21:30	3:30	3,9,11,13	12	4.7
	22:30	4:30			5.0
6 (50)	22:30	4:30	3,11,12,13	9	5.0
	23:20	5:20			5.5
7 (35)	23:20	4:30	3,11,12,13		5.5
	23:55	5:55pm			5.9

Notes:

1. Adjust Observing Schedule 4 min earlier for each day.
2. Sv 13 comes into view last and sv 6 sets first followed by sv 9.

The first few days of August were spent finalizing the test plan and mobilizing and testing of the various equipment required for GPS data collection from the oscillating mast assembly at the University of Calgary. A graduate student from the University Of Calgary was hired as an assistant for this experiment for equipment mobilization, GPS satellite receiver operation, and demobilization.

The first set of GPS data was collected using two TI4100 receivers from August 5 to August 8, inclusive. The second set of GPS data was collected from August 9 to 11 using two Norstar 1000 receivers modified for 5 Hz data output. Additional equipment used for the experiment included an HP220 computer for APR data collection, several Digi-Data tape cartridge recording units, and TI4100 GPS receiver power supplies consisting of two

12 volt lead acid batteries and charging units. The NS1000 receiver accepts 110 volt AC power which was available for this experiment.

A set of 8 four foot square reflector panels were fabricated using 2 mm thick aluminum sheets attached to half inch thick plywood. These sheets were used to induce multipath at the three remote antenna sites. The sheets were placed in a circular pattern around the pillar and red box antenna locations inclined approximately 45 degrees from horizontal (see photo in Appendix G). When the remote GPS antenna was located on the oscillating mast, the reflector sheets were placed in locations indicated in Figure 11. The exact locations were repeated during the mast observing periods while the other locations of the reflector sheets were only approximate.

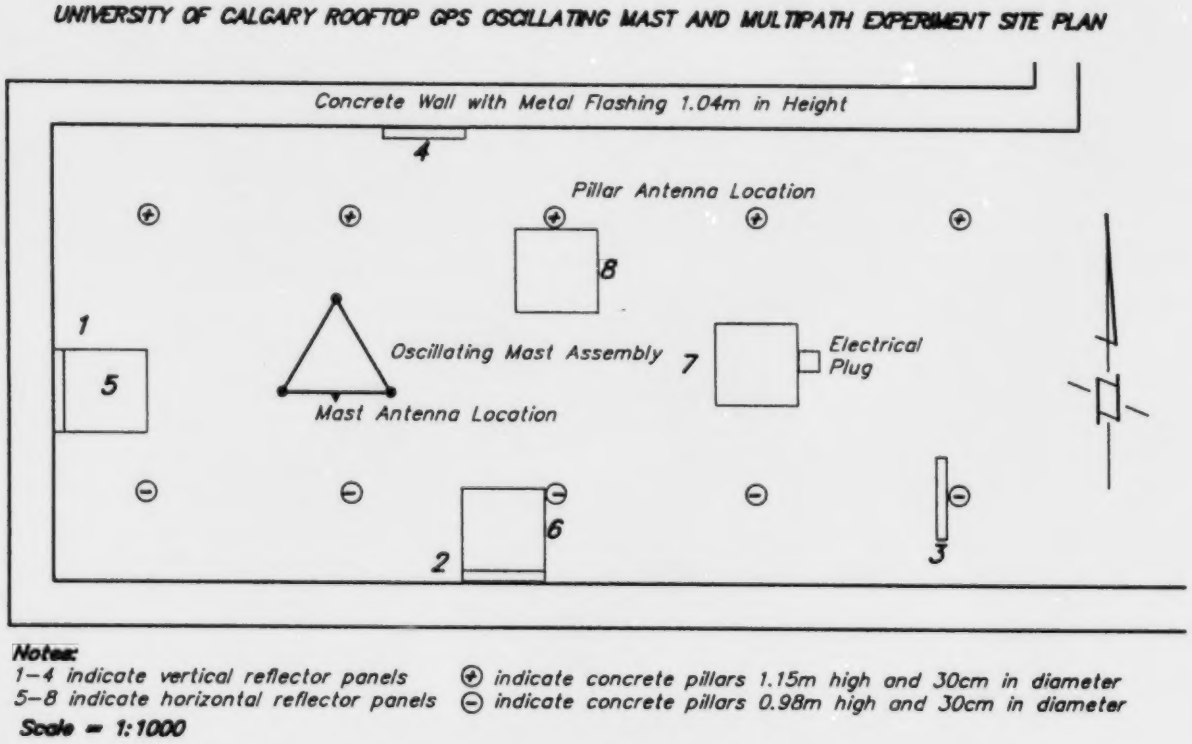

Figure 11. Oscillating Mast Experiment Site Plan

Some hardware problems were encountered in the first three days of observation with the TI4100 GPS receivers resulting in some data collection gaps. The major problem with the TI4100 receivers was CDU (Control Display Unit) lockup. This problem resulted in having to cold start the receiver which took approximately 30 minutes and the source of this problem was not completely resolved although it may have been due to static electricity.

An additional period of data was lost after a failure in a set of batteries due to a defective charging unit. It was decided to collect an additional day of TI4100 data to ensure an adequate amount of GPS data for analysis. The original intent was to collect C/A code data with the TI4100 receivers. Unfortunately the incorrect tracking mode was entered and P code L1 only data was collected instead.

The NS1000 receivers functioned very well with only few problems. One receiver had a defective AP (applications processor) board that resulted in a lockup condition when the receiver was in operation for more than four hours. This problem resulted in only a minor amount data loss at the end of the observing period and was verified to be temperature related using the Norstar temperature testing chamber.

Other problems encountered with the NS1000 receiver were due to AP software bugs and resulted in occasional 1 msec errors in pseudo range and 20 msec errors in phase. The pseudo range problem only occurred once and was corrected in real time by reacquiring the satellite and the phase data problem was corrected using a software patch. Since the test, both of these problems have been corrected by software upgrades from STI (Stanford Telecommunications Inc.), the manufacturers of the NS1000 receiver front end.

When the TI4100 receiver was first used it was apparent that a significant amount of jerk or bounce of the mast at the end of its swing arc was causing frequent and unacceptable cycle slips. This problem was found to originate with a worn gear in the mast drive mechanism and was avoided by slowing down the oscillation period to 20 seconds. A new gear box was installed on the oscillating mast assembly prior to the last day of TI4100 data collection (day 221) and the mast bounce problem was significantly reduced.

Overall the experiment was very successful in obtaining static and kinematic GPS data suitable for analysis and testing of the enhanced positioning algorithms and multipath effects. The new APR system (cf. Section 3.1.2), used to derive instantaneous mast positions and its associated real time software, functioned very well with no major problems. This resulted in an extremely accurate kinematic reference for determination of GPS positioning errors. Although some hardware problems were encountered with GPS data collection, more than enough good data was collected during the experiment. The oscillating mast experiment data collection summaries for the TI4100 and NS1000 receivers are contained in Tables 2 and 3.

Table 2. Mast Experiment TI4100 GPS Data Collection Summary

PERIOD	CODE	REMOTE LOC	PERIOD sec	REF	UD	REMARKS
1. AUGUST 5,DAY 218 Mast Length 4.27 m						
1						missed
2	P	mast	0	N	2	
3	P	mast	18	N	2	
4	P/L1	mast	0	N	2	
5	P/L1	mast	18	N	2	
6	P/L1	mast	18	Y	2	
7	P	mast	18	Y	2	
2. AUGUST 6,DAY 219 Mast Length 4.27 m						
1						missed
2						missed
3	P	pillar	0	Y	0	
4	P/L1	red box	0	Y	0	
5	P/L1	mast	18	Y	2	
6	P/L1	mast	18	Y	2	
7						missed
3. AUGUST 7,DAY 220 Mast Length 4.27 m						
1	P	pillar	0	Y	2	monitor battery
2	P/L1	red box	0	Y	1	failure, missed data
3	P/L1	red box	0	N	2	from 1:30 -> 2:16
4	P	mast	28	Y	2	
5	P/L1	mast	28	Y	2	
6	P/L1	mast	22	Y	2	
7	P	mast	22	Y	2	
4. AUGUST 8,DAY 221 Mast Length 4.27 m						
1	P/L1	pillar	0	Y	2	
2	P/L1	red box	0	Y	1	MON START 1:30
3	P/L1	red box	0	N	2	
4	P	mast	14	Y	1	
5	P/L1	mast	14	Y	2	MON NEW TAPE 3:40
6	P/L1	mast	18	Y	2	
7	P	mast	18	Y	2	

Table 3. Mast Experiment NS1000 GPS Data Collection Summary

PERIOD	REMOTE LOC	PERIOD sec	REF	UD	REMARKS
1. AUGUST 9,DAY 222 Mast Length 4.27 m					
1	pillar	0	Y	N	
2	pillar	0	N	N	
3	red box	0	Y	N	
4					missed
5	mast	14/28	Y	N	switch rec
6	mast	18	Y	N	
7	mast	14	Y	M	
2. AUGUST 10,DAY 223 Mast Length 4.27 m					
1	pillar	0	Y	N	
2	pillar	0	N	N	
3	red box	0	Y	N	
4	mast	14	Y	M	+/- 20 deg
5	mast	8	Y	M	
6	mast	17	Y	N	+/- 30 deg
7	mast	14	Y	N	
3. AUGUST 11,DAY 224 Mast Length 2.13 m					
1	pillar	0	Y	N	
2	red box	0	Y	N	
3	mast	13	Y	M	+/- 20 deg
4	mast	13	Y	W	
5	mast	13	Y	N	
6	mast	13	Y	N	+/- 30 deg
7	mast	8	Y	M	

3.2. RF Absorbent Ground Plane Experiment

After it was determined that there was significant multipath contamination of the pseudo range data collected from the monitor station during the oscillating mast experiment, the CHS requested that an additional experiment be performed to prove conclusively the effectiveness of multipath counter measures. J. Tranquilla from the University Of New Brunswick provided an RF absorbent ground plane to the University of Calgary. This ground plane, in conjunction with a single TI4100 GPS receiver, was used to conduct a multipath experiment over a period of three days in early November.

GPS pseudo range data was collected from the monitor location used for the previous oscillating mast experiment, using both the P and C/A code pseudo range tracking modes. This data was collected in five periods with and without the RF absorbent ground plane (cf. Table 4) from the same antenna location. All of the GPS data was collected using the 3 sec data rate provided by

the lowest tracking bandwidth (0.7 Hz) setting. The analysis of the data sets obtained from this experiment is contained in Section 4.2.

Table 4. RF Absorbent Ground Experiment TI4100 GPS Data Collection Summary

	PERIOD	CODE	GROUND PLANE	SV PRNS
1. November 6, 1988 Day 311				
1	13:05 13:30	P	Y	6,9,11,12
2	13:30 14:07	P	Y	6,11,12,13
3	14:07 15:05	P	Y	6,9,12,13
4	15:13 16:10	P	N	3,9,11,13
5	16:12 17:40	P	N	3,11,12,13
2. November 7,1988 Day 312				
1	12:52 13:25	P	N	6,9,11,12
2	13:25 14:05	P	N	6,11,12,13
3	14:05 15:13	P	N	6,9,12,13
4	15:13 16:06	P	Y	3,9,11,13
5	16:06 17:35	P	Y	3,11,12,13
3. November 8,1988 Day 313				
1	12:50 13:22	C/A	N	6,9,11,12
2	13:22 14:02	C/A	N	6,11,12,13
3	14:02 14:50	C/A	N	6,9,12,13
4	14:55 16:00	C/A	Y	3,9,11,13
5	16:00 17:15	C/A	Y	3,11,12,13

4. ANALYSIS OF RESULTS

4.1. Oscillating Mast Experiment

The next section describes how the data was processed and results obtained in deriving the reference positions. This is followed by discussion of the results obtained from the various multipath investigations. Finally the static and kinematic GPS positioning results obtained using various methodologies are discussed.

4.1.1. Establishment of Reference Positions

The processing of the mast data was initiated after collection and backup of the data to 9 track tape. First the required data to establish a control position for the monitor station, the remote observing pillar, and the mast was assembled from the first, second and third days of TI4100 GPS observations. The Nortech NOVAS (Nortech Vector Adjustment Software) program, which uses double difference GPS phase observations, was then run with the various data sets collected and preliminary positions for the three main stations used for the experiment were determined.

To determine a precise position for the monitor station at the U of C, simultaneous GPS data observed on day 220 at stations on our inertial baseline northwest of Calgary was used. These baseline stations (6 and 6A) were part of a larger network which had been previously determined using TI4100 receivers, NOVAS, and tied to a PZT station near Priddis. The corresponding NOVAS processing summaries are appended (Appendix E). TI4100 receivers were located at the U of C monitor station (UCM) and station 6, while a NS1000 receiver was used at station 6a. The triangle formed by these stations closed to within 7,7, and 10 mm in x,y and z (cf. Table 5). This misclosure accuracy is about 0.6 ppm and is well within expected solution accuracies obtained using static GPS phase data.

Table 5. U of C Monitor Station NOVAS Triangular Closure Summary

STATIONS	DX	DY	DZ
6 - UCM	2741.513	-19361.195	-13411.307
UCM - 6A	-2742.414	19362.892	13412.040
6A - 6	0.908	-1.690	-0.743
MISCLOSURE	0.007	0.007	-0.010

To derive the pillar station coordinates on the U of C roof a second set of NOVAS processing was done using dual frequency TI4100 data collected on day 219. The NOVAS solutions were gener-

ated using both L1 and L2 fixed integer solutions (Appendix E). Computation of the L1 and L2 baseline differences gives results of 7,30, and 33 mm in x,y,z. This accuracy is not what was expected over such a short baseline (over 1800 ppm) and indicates possible problems arising from multipath contamination of the phase measurements and differential antenna phase center variations. The apostori variance factor however was acceptable and the results from the L1 fixed integer solution were therefore used for the final pillar position.

TI4100 GPS data collected on Day 218 from the monitor station and mast (while it was stationary) was used to derive the oscillating mast reference position. This was a limited data set with very poor NOVAS results (cf. Appendix E). To verify the mast reference position, a conventional survey was conducted in late December. This was performed using a WILD T2000 total station electronic theodolite with a DI2000 infrared distance measurement unit. The monitor station and the pillar stations were occupied and horizontal angles, vertical angles, and slope distances were measured to a target on the mast.

The network adjustment was performed using the IBM PC based program named GEOLAB, developed by BitWise Ideas Inc. Due to the questionable quality of the vertical angles, identified in the initial adjustment by the observation residuals, it was necessary to use fixed heights and perform a second two dimensional horizontal adjustment. Since there was an accurate measurement on the height of the mast rotational center with respect to the height of the observation pillar, the difference in these heights was used to fix the mast elevation. The values of the mast to pillar height difference from ground truth and the initial GEOLAB adjustment was 1.4 cm. The differences between the initial and final GEOLAB adjustment latitude and longitude values were less than a millimetre.

The final GEOLAB conventional coordinates and the GPS NOVAS derived coordinates for the mast location differed by -0.215, 0.026 and 1.040 metres in latitude, longitude, and height respectively. The complete GEOLAB listings for the initial 3-d and final 2-d adjustments used in determination of the oscillating mast center of rotation, are contained in Appendix E. The final control positions for the monitor station and the remote pillar and mast locations are summarized in Table 6.

Table 6. U of C Mast Test Station Final Coordinate Summary

STATION	WGS-84 COORDINATES	UTM COORDINATES
MONITOR	N 51 04 45.947 W 114 07 56.704 1117.177	5662569.843 700855.733
PILLAR	N 51 04 45.936 W 114 07 57.955 1116.214	5662568.555 700831.411
MAST (Center of Rotation)	N 51 04 45.849 W 114 07 58.123 1116.794	5662565.741 700828.247

DAY	MONITOR ANTENNA HEIGHT	MAST ANTENNA HEIGHT
218	1118.687	1121.066
219	1118.690	1121.066
220	1118.720	1121.066
221	1118.709	1121.066
222	1118.679	1121.066
223	1118.633	1121.066
224	1118.649	1118.929

4.1.2. Multipath Analysis

4.1.2.1. Phase Smoothed and Pseudo Range Differences

Using the method of raw pseudo range and phase smoothed range comparison, an extensive review of existing data collected under both static and kinematic conditions was performed. The oscillating mast experiment provided a large amount of GPS static data collected while measures were taken to induce multipath. Both P and C/A pseudo range multipath contaminated data were collected from the following static sites:

1. a roof top monitor station with a number of metal heating vents with convex surfaces to the north-west (see photos in Appendix G):

2. a concrete pillar 1.15 m in height and 30 cm in diameter surrounded by 8 reflector sheets,

3. an oscillating mast 6 metres (4 metres on day 224) from the roof surrounded by 8 reflector sheets, and

4. red wooden box 30 cm high with multipath sheets.

A polar visibility plot, generated using an alert generation program is illustrated in Figure 12. The satellites for the most part are to the south when at low elevations with the exception of Prn 11 which is setting to the east and Prn 12 which is rising from the west. This means that any obstructions or reflecting surfaces to the North will not affect the direct signal, however, they will provide a good back ground surface for multipath generation.

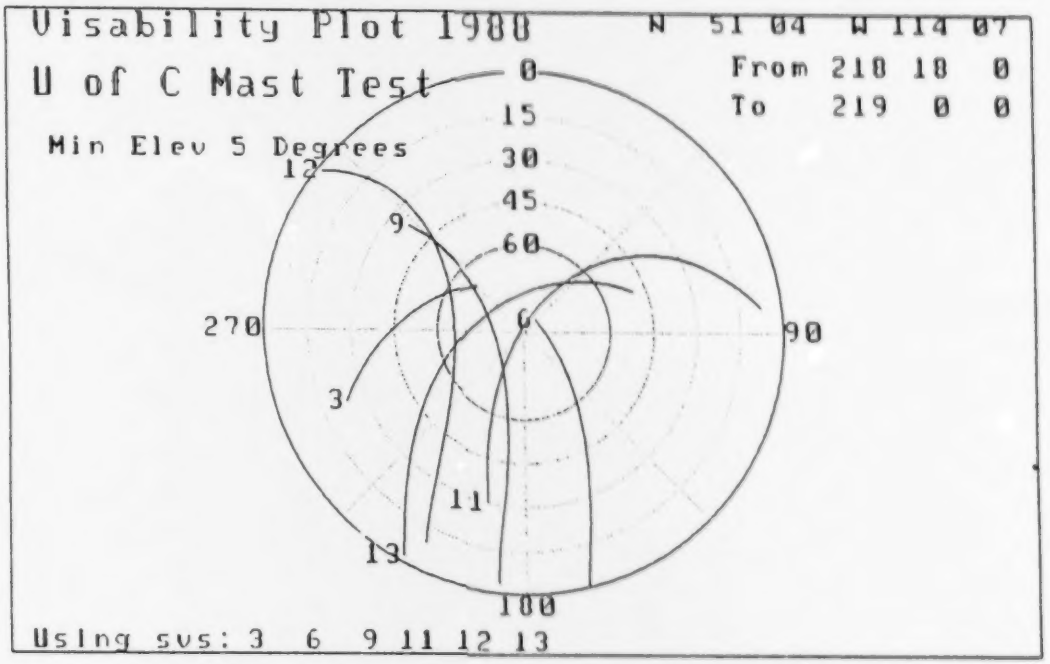

Figure 12. Polar Visibility Plot Day 218, 1988 U of C
Note: Location Of SV Prn Number Indicates Starting Position

There was no appreciable pseudo range multipath detected from analysis of the kinematic data collected from the mast either in P or C/A code tracking modes (cf. Figure 13). The monitor station gave the most multipath as illustrated in Figures 14, 15, and 16. The periods of the highest magnitude variations varied from 30 seconds to 10 minutes. The multipath repeatability between successive days due to a high correlation is clearly seen when comparing Figure 14 and 16 then the P code was used. The multipath is not exactly the same due to the slightly different antenna heights between successive days of observation (cf. Table 6). The maximum amplitude of the multipath was 8 to 10 metres.

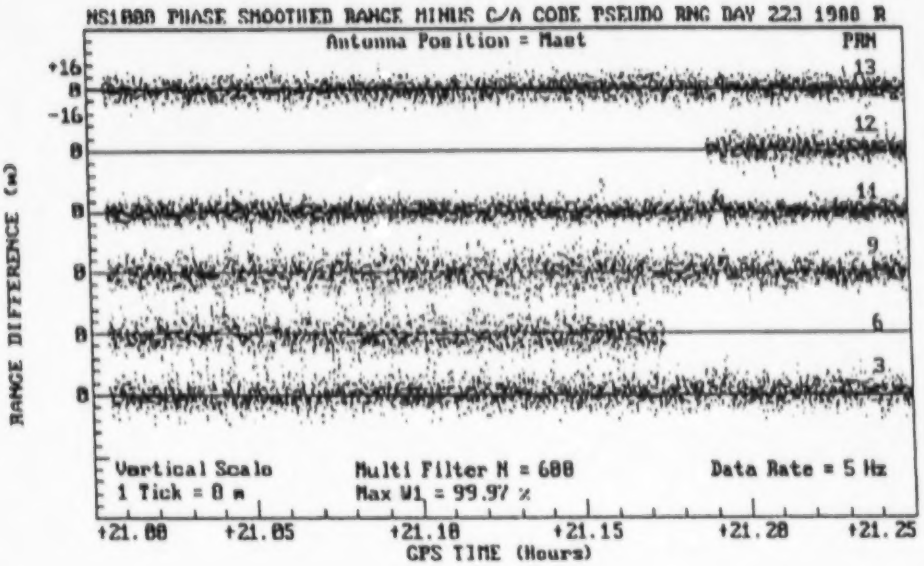

Figure 13. Day 223 Oscillating Mast Kinematic Raw Pseudo Range Minus Phase Smoothed Range Variations

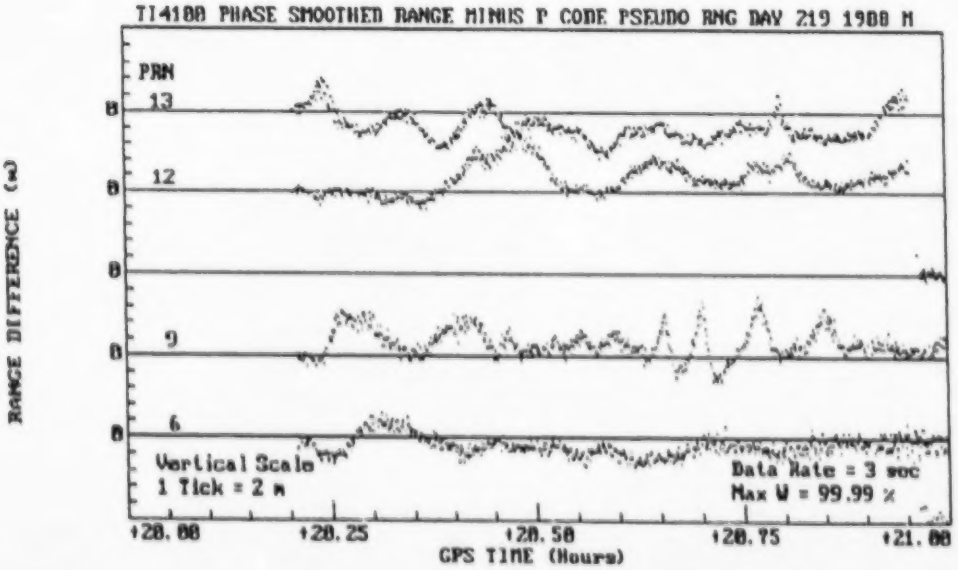

Figure 14. Monitor Station Day 219 P Code Multipath

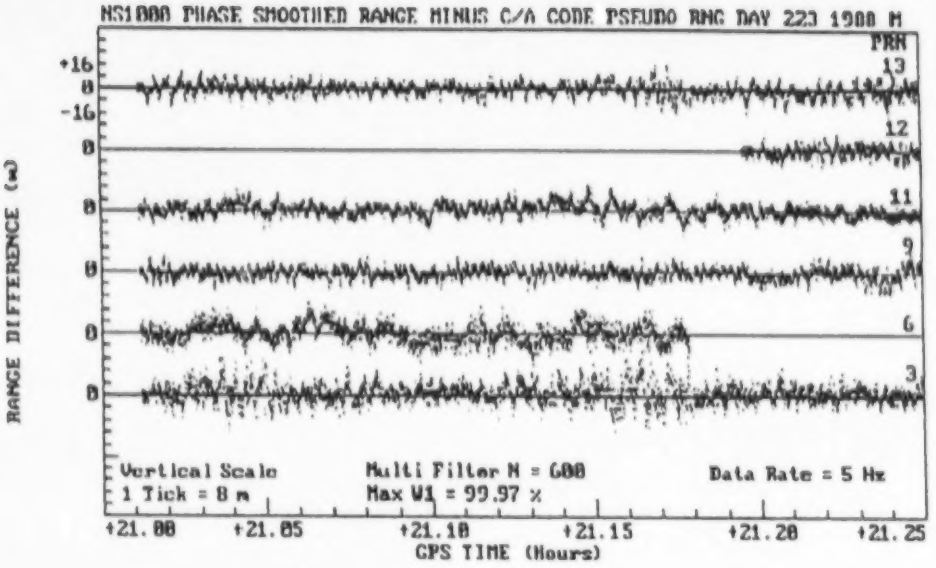

Figure 15. Monitor Station Day 223 C/A Code Multipath

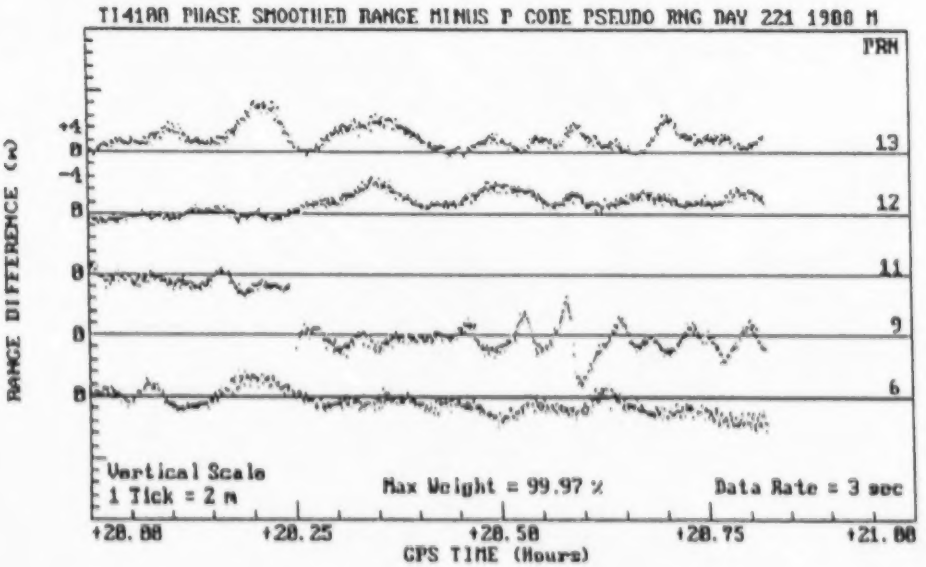

Figure 16. Monitor Station Day 221 P Code Multipath

A previous analysis of noise levels present in GPS data collected in static and dynamic cases was conducted under this contract (cf. May 31 Progress Report). It was found that low multipath static sites had P and C/A code noise levels of 0.5-0.9 metres and 2-4 metres respectively. Static sites with high multipath exhibited P and C/A code noise levels of 1.0-2.0 metres and 4.0-6.0 metres respectively. Kinematic P and C/A code noise levels were found to be around 1 metre and 4-6 metres respectively. After a comparison of the pseudo range noise levels found in this experimental data, it is concluded that they are very similar in magnitude (cf. Table 7).

Table 7. Summary Of Mast Experiment Pseudo range noise levels

PERIOD		CODE	LOCATION	Av.Std.Dev.	Samples	Bandwidth
August 5, 1988 Day 218						
1	19:45 20:20	P	Mast(Static)	1.038	6272	UD2
2	20:20 21:00	P	Mast	1.034	7238	UD2
August 6, 1988 Day 219						
1	20:12 21:00	P	Monitor	1.657	3692	UD0
2	20:12 21:00	P	Pillar	0.658	3575	UD0
August 7, 1988 Day 220						
1	19:00 23:12	P	Monitor	1.592	19090	UD0
2	19:10 20:48	P	Pil.& R.Bx.	1.519	14556	UD2,1,2
August 8, 1988 Day 221						
1	19:00 19:30	P	Monitor	1.321	2131	UD0
2	19:00 20:48	P	Monitor	1.735	7665	UD0
3	21:30 23:45	P	Monitor	1.351	8816	UD0
4	19:00 21:00	P	Pil.& R.Bx.	1.027	15750	UD2,1,2
August 9, 1988 Day 222						
1	18:30 23:30	C/A	Monitor	4.318	7974	N
August 10, 1988 Day 223						
1	18:30 19:06	C/A	Monitor	5.532	48479	N
2	18:05 19:00	C/A	Pillar	3.950	44932	N
3	20 54 23:30	C/A	Mast	5.194	40615	M&N
August 11, 1988 Day 224						
1	18:30 19:30	C/A	Monitor	4.692	8704	N
2	20:00 20:30	C/A	Monitor	4.017	52025	N
5	18:30 19:30	C/A	Pillar	3.072	17569	N
3	20:00 20:30	C/A	Mast	5.124	42755	M

Monitor station multipath variations, particularly those generated with P code data, were very repeatable and had very long periods of 5-10 minutes and amplitudes reaching 8 to 10 metres. C/A code noise levels averaged around 5 metres rms for both mast and monitor station data. Closer inspection of the data graphs however, reveals multipath with periods ranging from 10-20 seconds to 2 minutes with amplitudes as high as 20 metres. Pillar and red box P code multipath statistics generated, indicated much lower pseudo range noise levels (0.5 to 1.5 metres) with less pronounced multipath variations (cf. Figure 17). A possible explanation for the difference in magnitude is the proximity of the reflector sheets (1-3 metres) compared to the convex surfaces of the heating vents at the monitor station (5-10 metres). Another observation site difference was the relative location of the metal flashing around the outside edge of the roof. With the monitor station this source of reflection was located 1.5 metres below the antenna and further away than with the pillar station. (see photos in Appendix G). Similar reductions in multipath were observed at the pillar with C/A code data as illustrated in Figure 18.

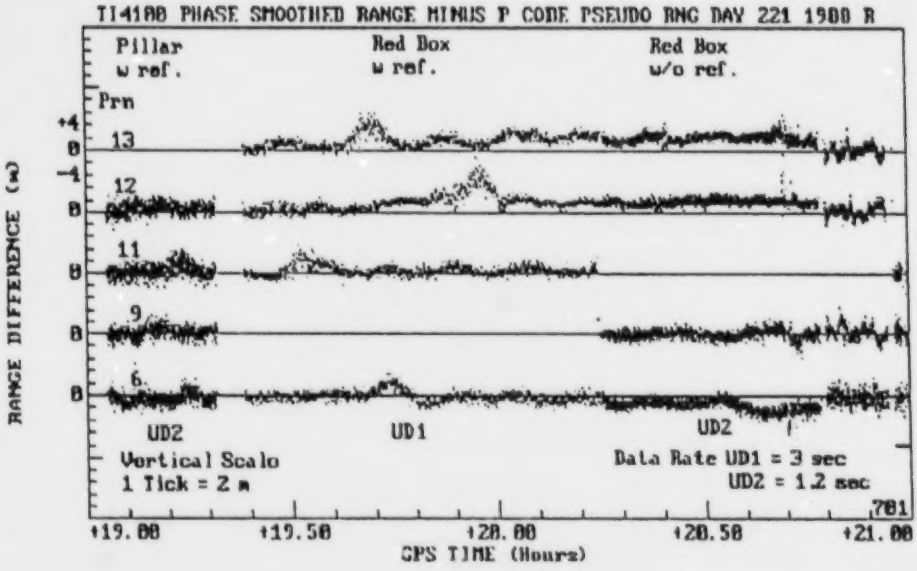

Figure 17. Pillar and Red Box Multipath P Code Example Day 221

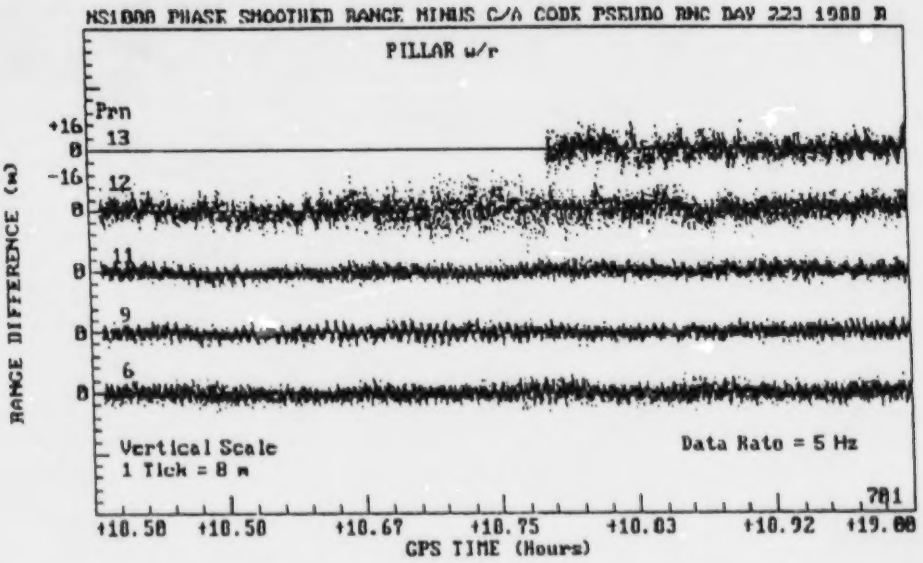

Figure 18. Pillar Multipath C/A Code Example Day 223

4.1.2.2. Signal Strength Variations

Another method of deriving information about multipath, at a stationary observation site, is by examination of the signal strength variations. As illustrated in Figure 19, multipath phenomena introduces significant signal strength deviations similar in period to the large multipath phenomena. Comparison with Figure 16 reveals the strong correlations with P code pseudo range multipath periods. Similar short and long term variations were also observed with the NS1000 monitor station data as illustrated in Figure 20. Comparison with Figure 13 reveals similar long term multipath induced variations in both signal strength and pseudo range noise levels (e.g. Prn 3 has increased pseudo range noise levels at 21.04 and 21.16 hours (Figure 15) which correspond to lower signal strength levels (Figure 20)).

The remote kinematic station signal strength characteristics are however much different (cf. Figure 21). It is apparent that low elevation satellites exhibit much noisier signal strengths with some additional variations due to motion, resulting from changes in the antenna's local horizon, and to a lesser extent due to non-symmetric antenna gain pattern (e.g. SV 6 is setting to the south and is below 10 degrees elevation while Sv 11 is at 70 degrees elevation).

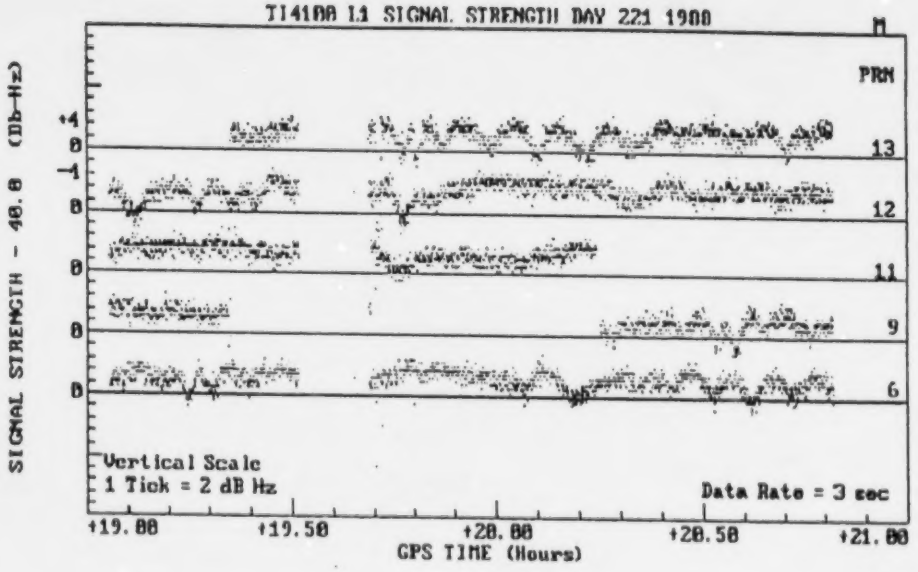

Figure 19. Mast Experiment P Code Monitor Station Signal Strength Variation Graph Day 221

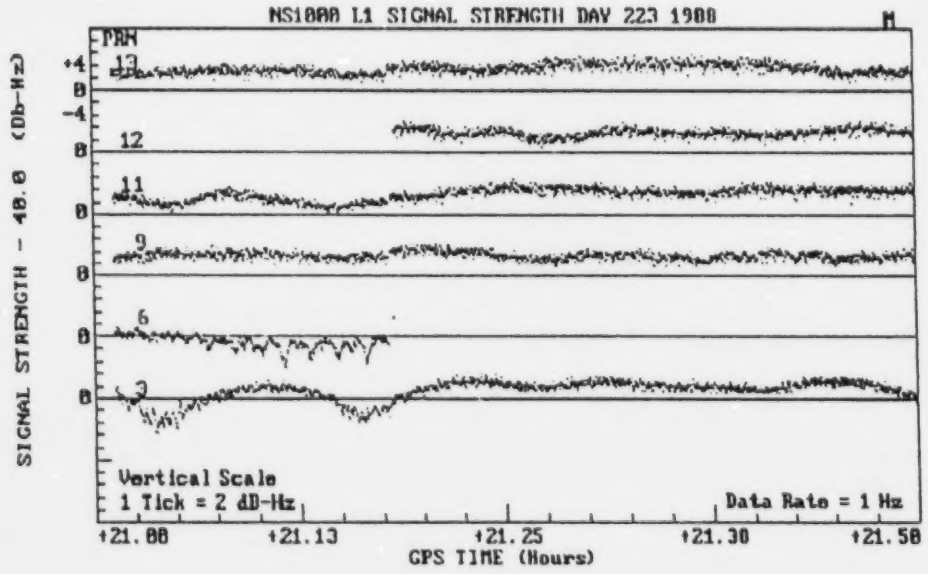

Figure 20. Mast Experiment C/A Code Monitor Station Signal Strength Variation Graph Day 223

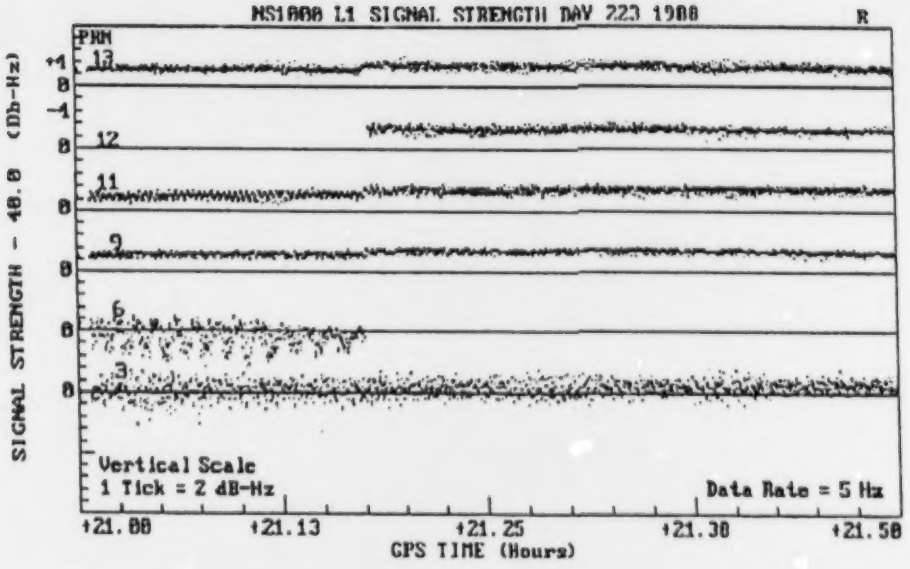

Figure 21. Mast Experiment C/A Code Mast Station Signal Strength Variation Graph Day 223

4.1.2.3. Fourier Analysis

An analysis of multipath induced pseudo range noise, using the Fourier transform as a methodology to filter out the high frequency noise, was performed using the mast experiment data. Both C/A and P code multipath correlations at the various static observation sites were conducted. The correlations using this method exhibit some interesting characteristics particularly in the similarities of their frequency spectra. Figure 22 illustrates a typical C/A code stationary site frequency spectra with the lower period (multipath) components much larger in amplitude than the higher frequency (noise) components. C/A code multipath for a similar period the proceeding day (time shifted 4 minutes earlier) also exhibits similar low frequency increases in amplitude (Figure 23).

The correlation of FFT filtered C/A code monitor station range data contaminated with multipath errors, was successful as illustrated in Figure 24. The spectral characteristics are nearly identical for the satellite pairs, but do vary quit significantly between the different satellites. The other satellite filtered range correlations exhibit similar magnitudes of about ±10 metres and were subject to some minor uncorrelated variations (cf. Appendix E). This may be partly attributable to the slightly different monitor station antenna placement between the two days of data (e.g. Day 224-223 = 1.6 cm in height; cf. Table 6).

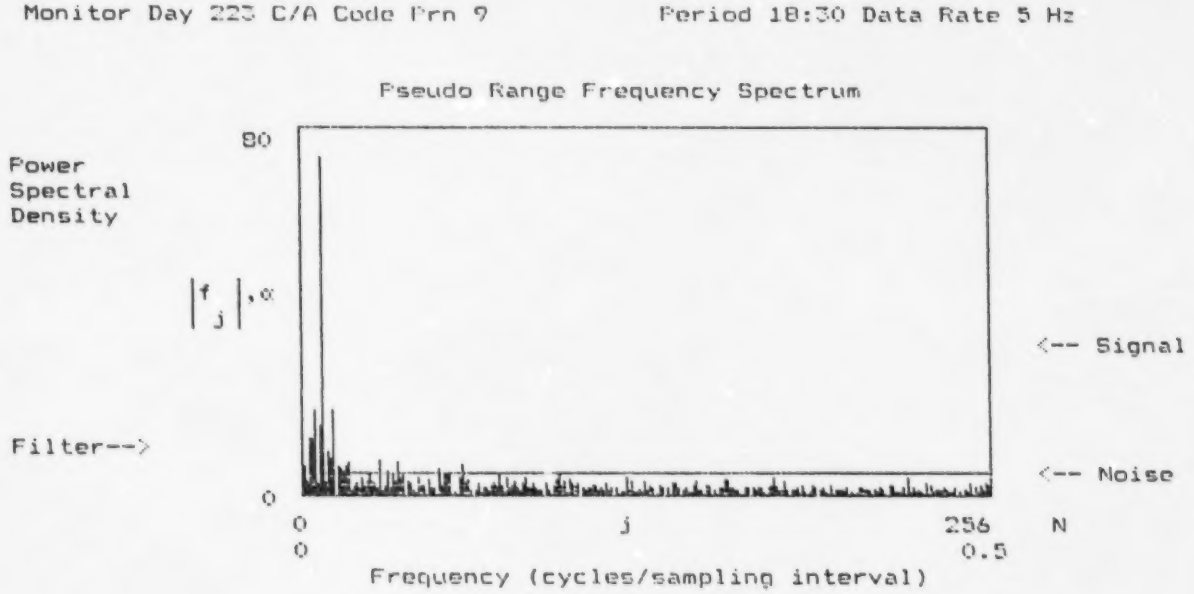

Figure 22. MCAD Multipath C/A Code Frequency Spectra Monitor Station Day 223 Prn 9 Start Time 18:30

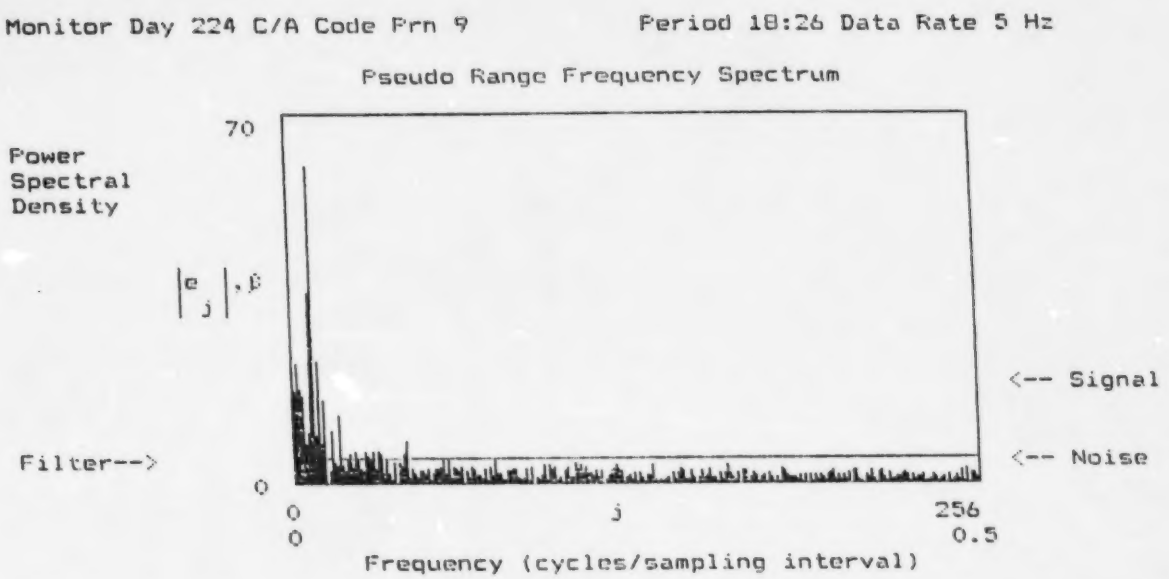

Figure 23. MCAD Multipath C/A Code Frequency Spectra Monitor Station Day 224 Prn 9 Start Time 18:26

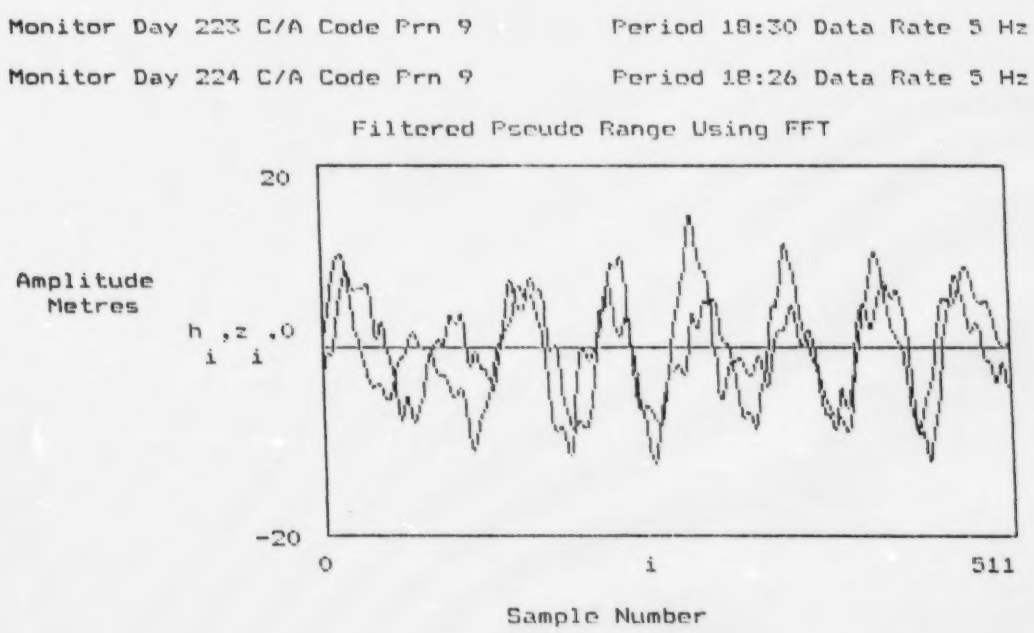

Figure 24. MCAD Multipath C/A Code Filtered Correlations Day 223/224 Monitor Station Prn 9

The kinematic mast FFT analysis revealed some very interesting differences from the static station data both in the flatter frequency spectra (Figure 25) and the resultant filtered range noise levels. The frequency spectra for most of the satellites was very flat resulting in a decrease in peak to peak noise levels after filtering (from 20-30 metres down to 5-10 metres (cf. Appendix E). There were however some slight differences in the spectral representations between different satellites particularly due to low elevation observation angles which showed up as increased amplitudes of the lower frequency components.

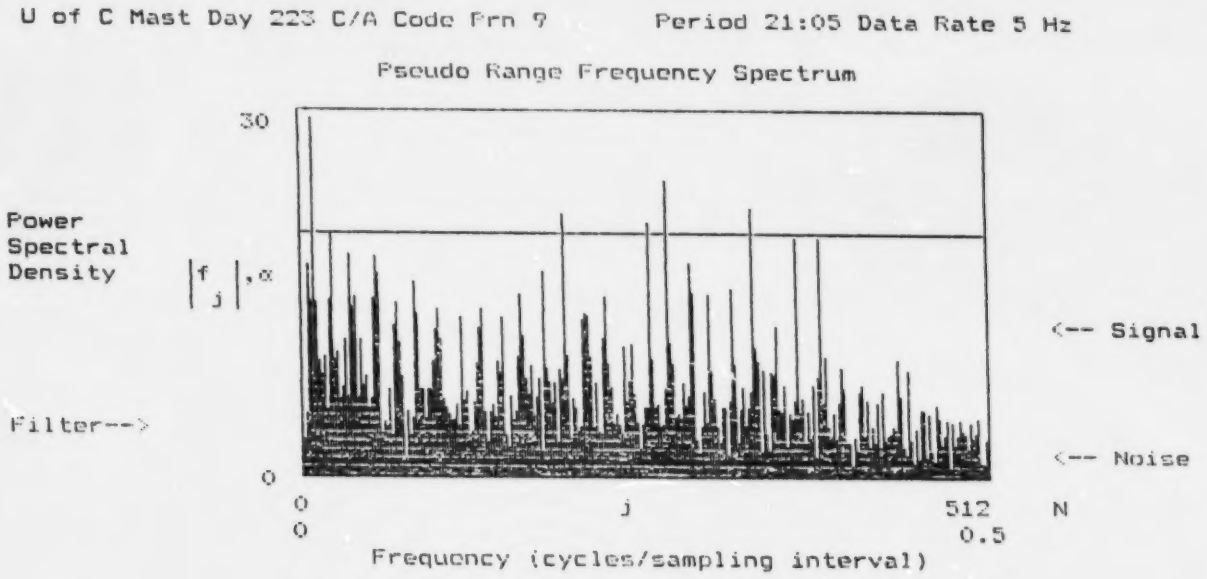

Figure 25. MCAD C/A Code Frequency Spectra Kinematic Mast Day 223 Prn 9 21:05

Pillar and red box multipath analysis using P code data from days 220 and 221 was also performed (cf. Figures 26 and 27). Time shifted satellite range frequency distributions showed similar spectral components, however general high frequency noise amplitudes had significant variations that were not confined to a single day or satellite. The resulting pillar and red box range correlations were weaker with some similar filtered variations apparent between satellite pairs. These results can be explained by the slightly dissimilar reflector panel placement from day to day and illustrates the sensitivity of multipath phenomena to local receiving environment differences.

Pillar w/r Day 221 P Code Prn 11 Period 19:07 Data Rate 1.2 sec

Pillar w/r Day 220 P Code Prn 11 Period 19:11 Data Rate 1.2sec

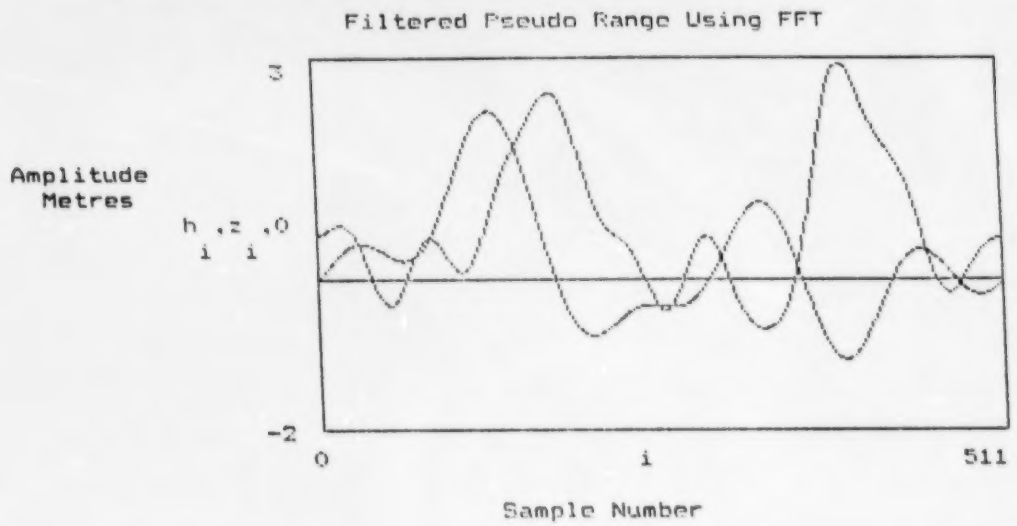

Figure 26. MCAD Multipath P Code Filtered Correlations Day 220/221 Pillar Station With Reflectors

Red Box w/r Day 220 P Code Prn 6 Period 19:27 Data Rate 3 sec

Red Box w/r Day 221 P Code Prn 6 Period 19:23 Data Rate 3 sec

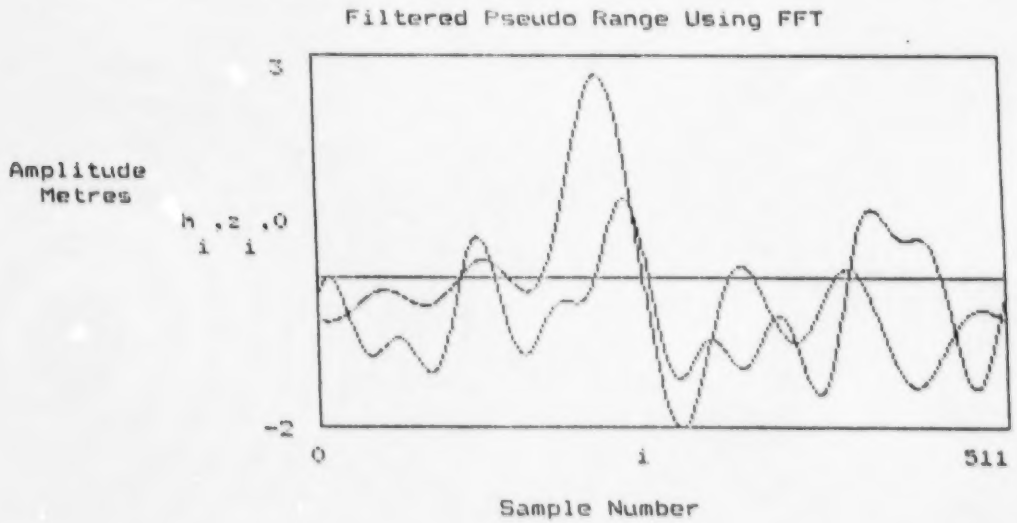

Figure 27. MCAD Multipath P Code Filtered Correlations Day 220/221 Red Box Station With Reflectors

Analysis of C/A code multipath phenomena for the pillar station without reflector panels was performed using data from days 222 and 223. The results of the frequency spectra comparisons and filtered pseudo range variations were highly correlated for certain satellites and weaker for others. Figures 28 and 29 illustrate the high correlations for satellite 9 in frequency spectra. As with other pillar and red box data collected with and without reflectors the general noise levels between days were dissimilar. The predominant multipath induced low frequency spectral components however exhibited a high degree of correlation. The resulting filtered pseudo range differences also exhibited a high degree of similarity as illustrated in Figure 30.

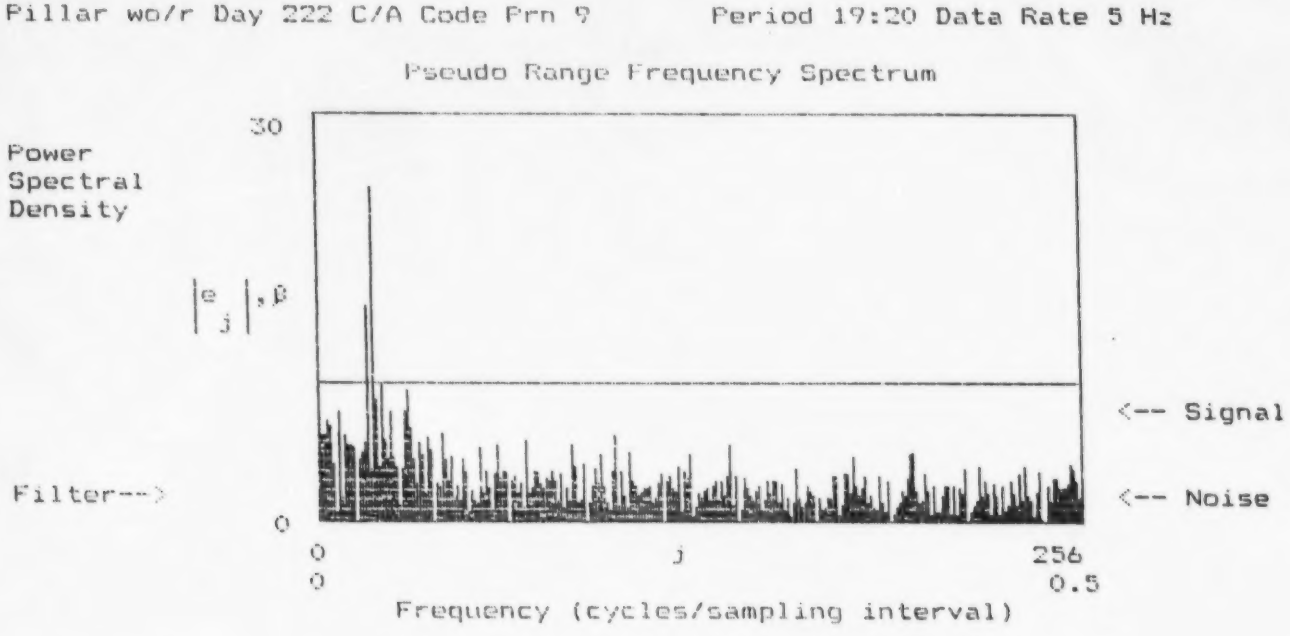

Figure 28. MCAD Multipath C/A Code Frequency Spectra Day 222 Pillar Station Without Reflectors

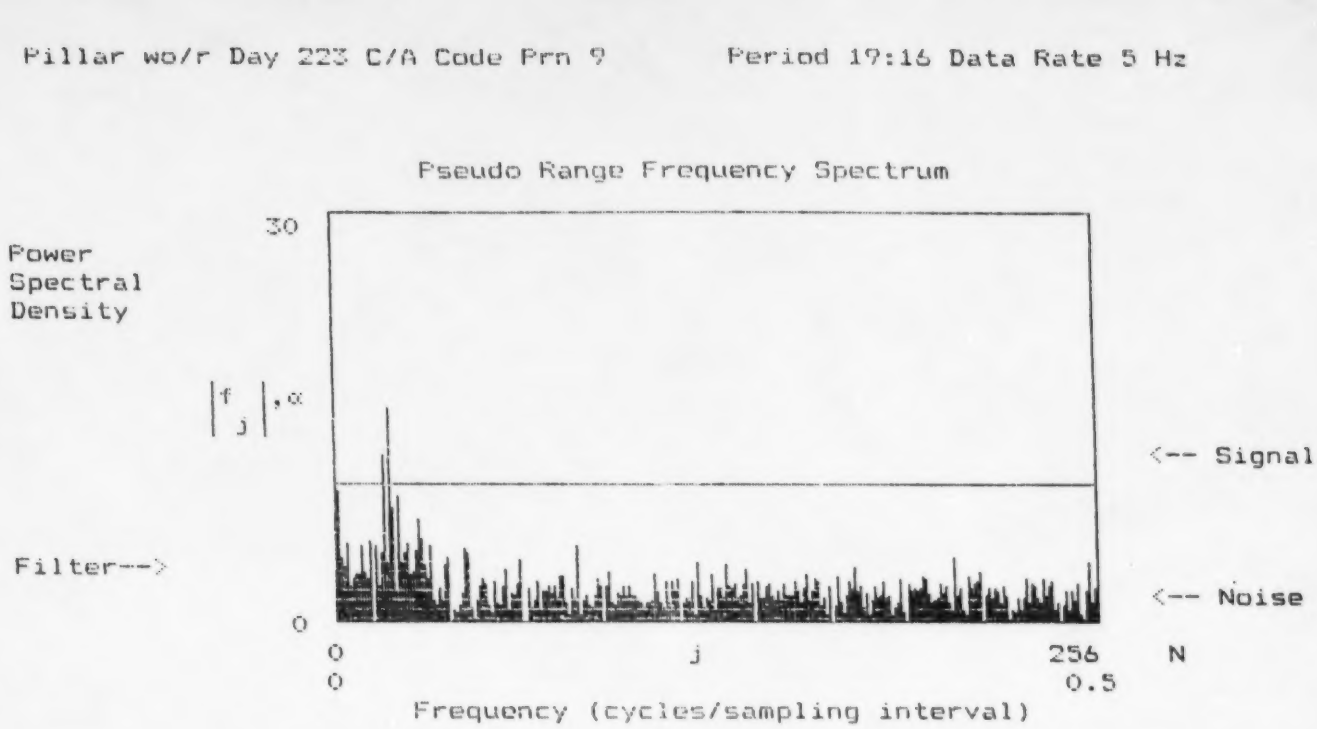

Figure 29. MCAD Multipath C/A Code Frequency Spectra Day 223 Pillar Station Without Reflectors

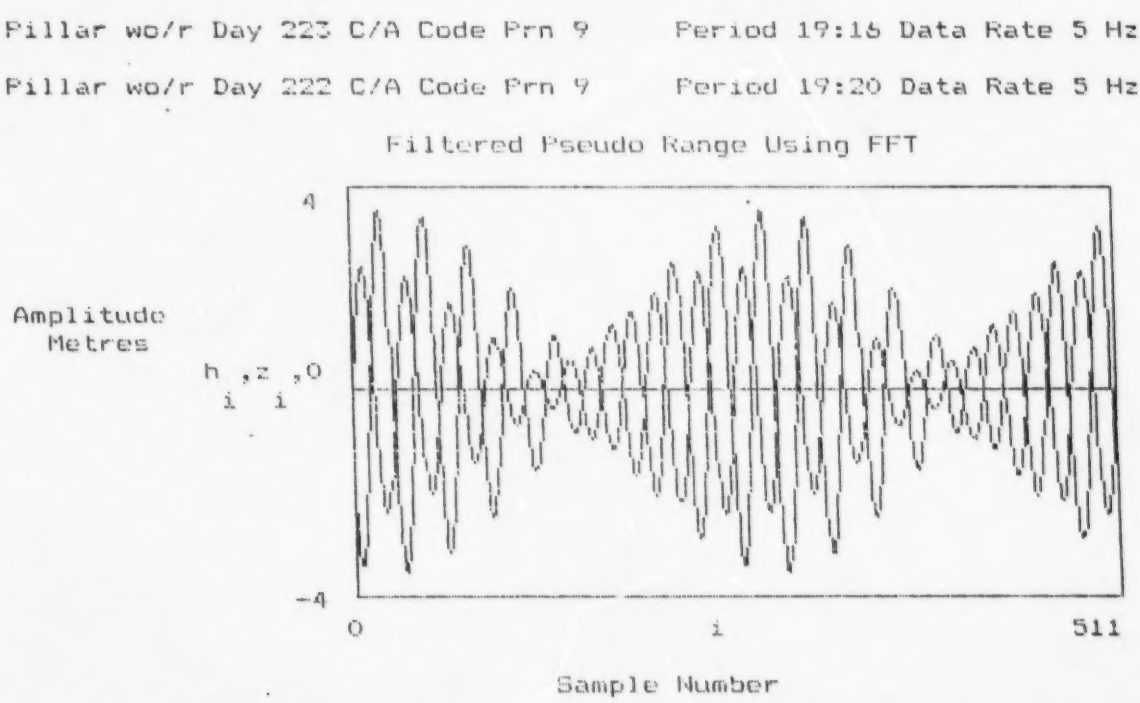

Figure 30. MCAD Multipath C/A Code Filtered Correlations Day 222/223 Pillar Station Without Reflectors

4.1.3. GPS Positioning Results

The following section reviews the processing methodology in deriving both static and kinematic position differences. For this analysis, both the multi-filter pseudo range method and the Discrete Relative Phase (DRP) method were used.

4.1.3.1. Static GPS Positioning Results

Using a specially modified version of HYDROSTAR running on a IBM PC compatible and written in the "C" programming language, the following position data was generated. The first set of program modifications involved multi-filter implementation as discussed in Section 2.3. The second involved the DRP method of using 100% phase to generate GPS differentially corrected positions.

Multi-filter pillar positioning results (Figure 31) were generally poor due to the combined effects of multipath at the monitor and remote stations. A filter count of 600 was used to bridge multipath of 2 minutes in duration and low elevation sv de-weighting was enabled. Height differences (±4m) are similar to Northing and Easting differences with discontinuities arising from occasional monitor station filter resets. Figure 32 illustrates these resets and residual multipath contamination present in the differential corrections (1-2m).

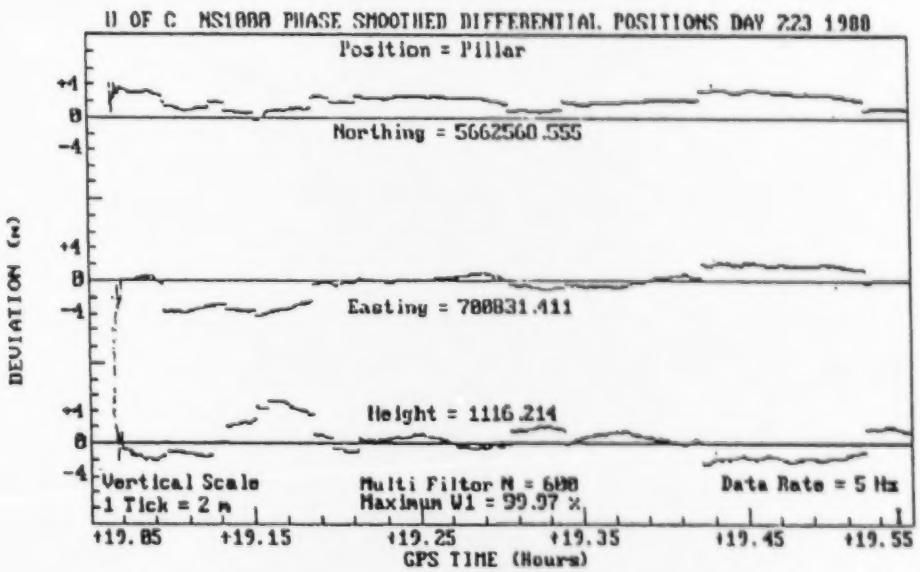

Figure 31. NS1000 Static C/A Code Multi-Filter Position Deviation Graph Pillar Day 221

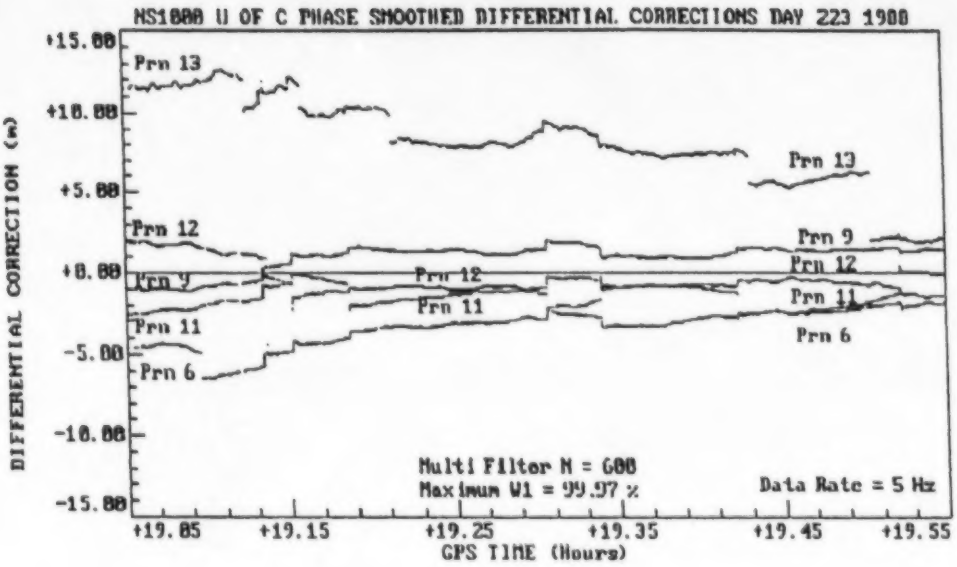

Figure 32. NS1000 Monitor Station Multi-Filter Differential Correction Graph Day 221

The DRP 100% phase pillar positioning results, as illustrated in Figures 33 and 34, have much smaller and very similar multipath induced deviations with maximum peak to peak variations of ±4 cm. The major source of multipath is confirmed by examination of the corresponding differential correction graphs (Figures 35 and 36). There are however some common pillar station induced multipath effects as found in previous MCAD multipath analysis (section 4.1.2.3).

The TI4100 position data has slightly higher noise levels than the NS1000 data which is most likely due to the different antenna phase center variations (cf. Nortech, 1987) and number of satellites being tracked. Other possible sources of the higher noise levels may be due to the difference in tracking bandwidths (UD2 = 8.0 Hz and NARROW = 5 Hz) and the differences in internal receiver phase tracking methods (i.e. the TI4100 uses single channel multiplexing and the NS1000 has 5 dedicated channels). Height and Easting seem to be affected more than Northing which is due to both the difference in geometrical strengths of the solution components and the particular satellites being affected by multipath (i.e. GDOP varied from 5.4 to 6.8 for 4 sv's, and 4.4 to 4.9 for 5 sv's).

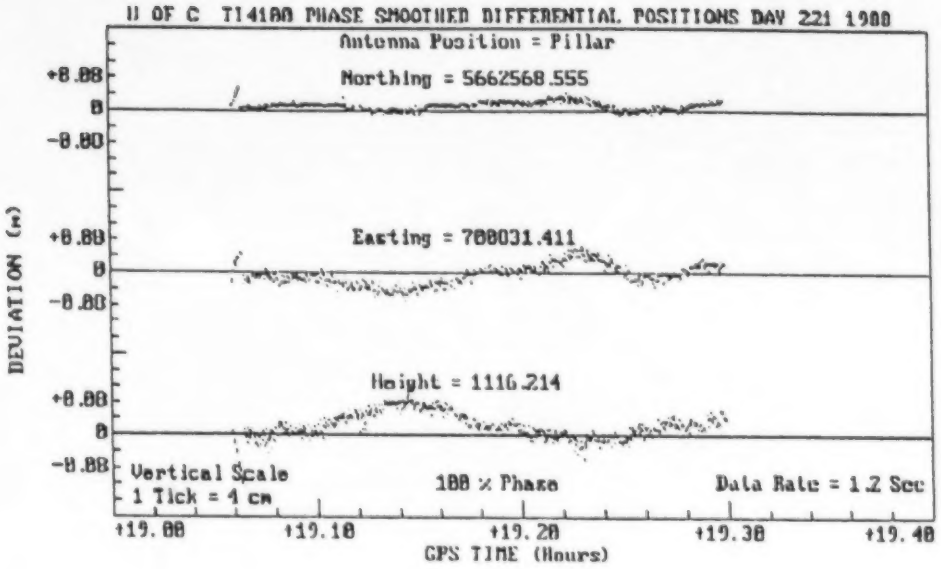

Figure 33. DRP 100% Phase Position Deviation Plot For Pillar Day 221

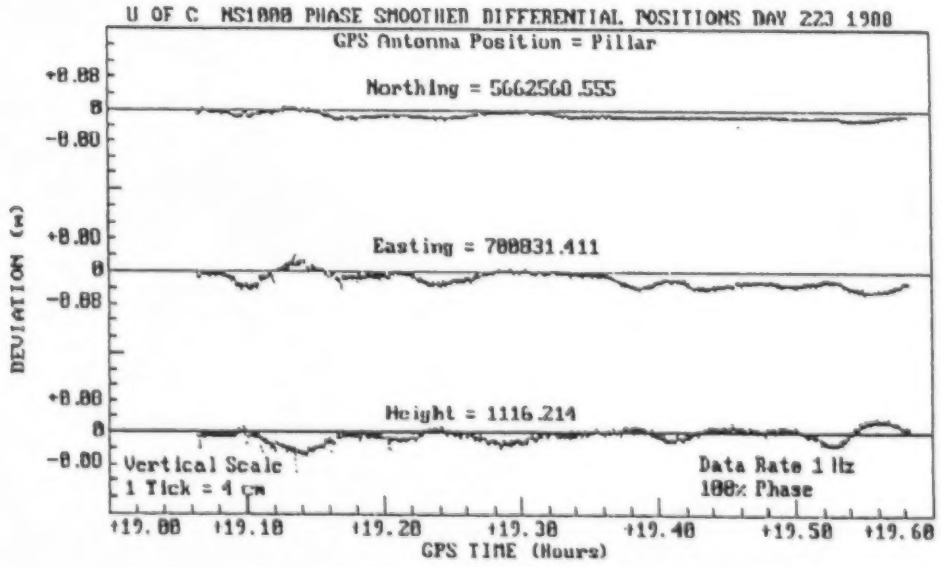

Figure 34. DRP 100% phase Position Deviation Plot For Pillar Day 223

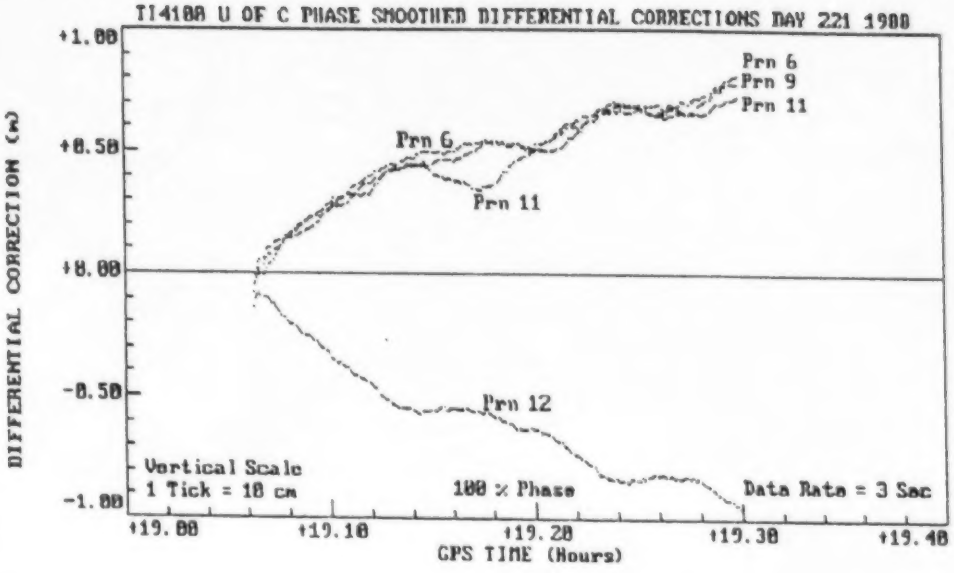

Figure 35. DRP 100 % Phase Differential Corrections For Monitor Day 221

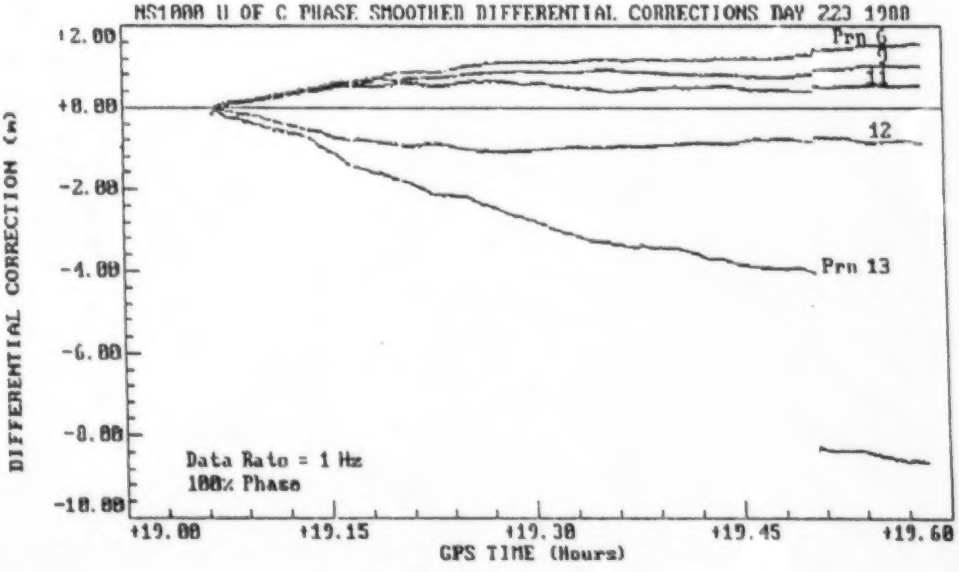

Figure 36. DRP 100 % Phase Differential Corrections For Monitor Day 223

4.1.3.2. Kinematic GPS Positioning Results

Multi-filter kinematic positioning results were generated using both P code and C/A code GPS data sets . The maximum filter counts used were 600 and 300 to effectively bridge multipath variations of 2 minutes with NS1000 5 Hz C/A code data sets and to a maximum of 15 minutes with TI4100 3 second monitor station P code data. The ionospheric de-weighting option was enabled for some of the data sets (e.g. Day 223) where low elevation (less than 15 degrees) satellites were used. Both the monitor and remote stations were processed using identical range weighting options and no data decimation options were used.

P code results obtained from Day 221 (Figure 37) are very good with deviations in Easting and Northing position components from reference positions of -0.8 m and +1.5 m respectively. Height of the oscillating mast is consistently low from -0.4 m to -1.0 m with no major deviations after filter stabilization. Growth in errors after filter stabilization is minimal for all three coordinates and is related to geometry effects arising from the pseudo range and phase integration filter locking into a slightly incorrect integer ambiguity on one or more satellite ranges.

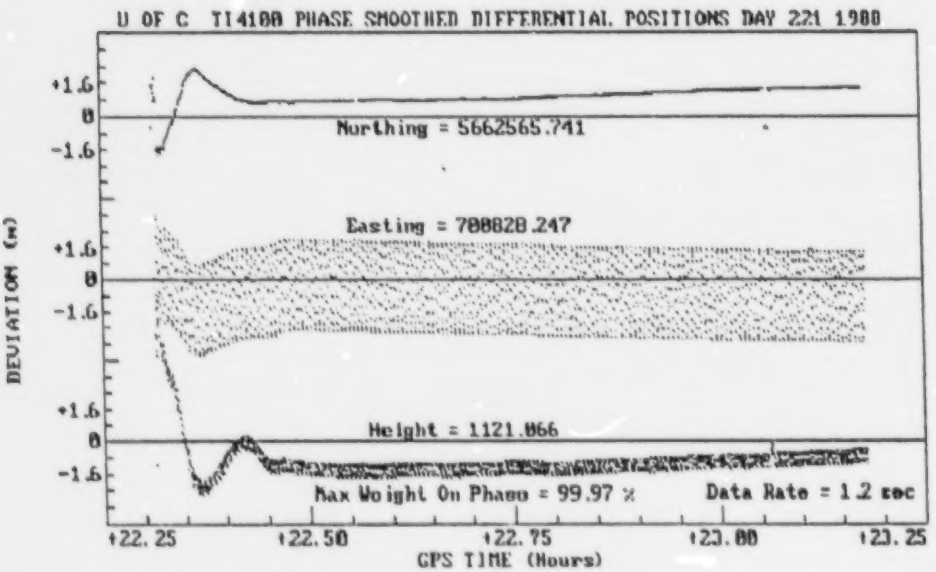

Figure 37. Day 221 P Code Kinematic Multi-Filter Position Graph

C/A code kinematic position results were generated for Days 223 and 224. Day 224 data (Figure 38) had systematic deviations in the Easting and Northing position components from reference positions of approximately +0.8 m and +1.2 m respectively. Height of the oscillating mast is consistently low from -0.8 m to -2.4 m with major deviations after filter stabilization. The small long period deviations in the positions are due to monitor station multipath effects contaminating the differential corrections (cf. Figure 39). The low frequency oscillations in the height from 20.3 to 20.45 hours are due to similar problems with the differential correction from satellite 13 which decreases from 0.50 m to -1.0 m over the same period. Slightly less stable C/A code results are therefore attributable directly to monitor station multipath contamination.

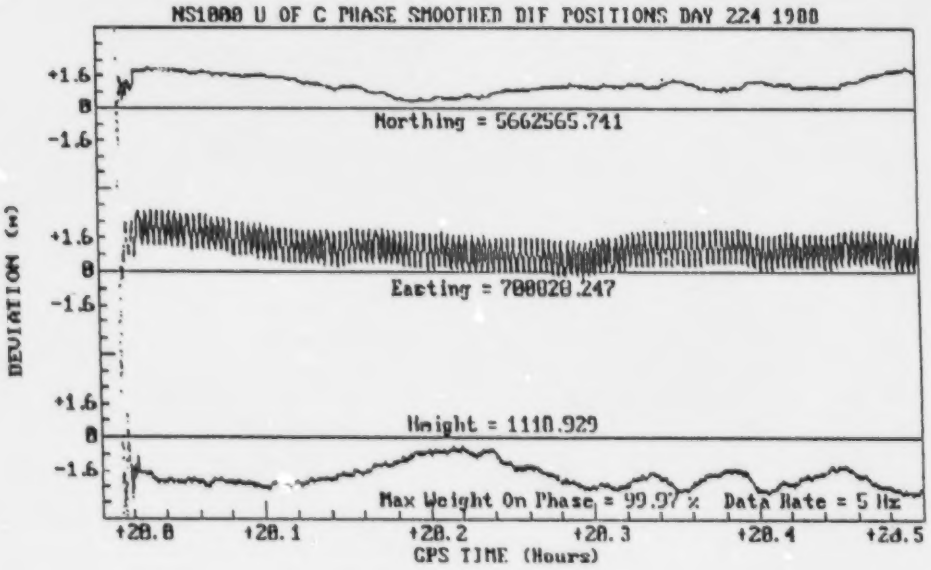

Figure 38. Day 224 Multi-Filter Kinematic Position Graph

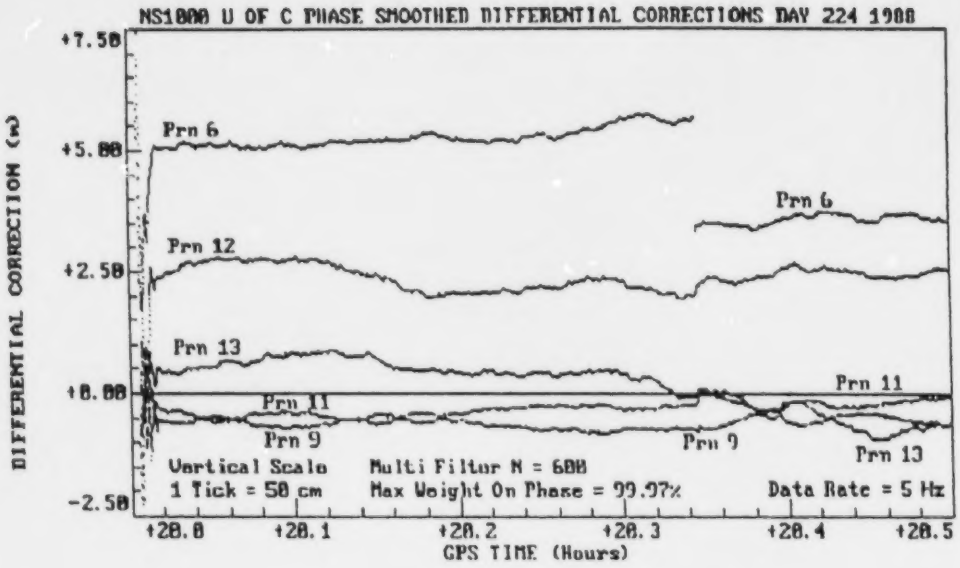

Figure 39. Day 224 Multi-Filter Differential Correction Graph

Day 223 position results, generated with a multi-filter option and low elevation phase de-weighting introduced through the ionospheric phase advance variance term, are illustrated in Figure 40. The first two discontinuities in height are related to cycle slips on satellite 6 which is below 7 degrees in elevation and decreasing. The next discontinuity is due to a satellite constellation change (i.e. Prn 6 is dropped and Prn 12 is acquired). Both position biases and long period fluctuations are greater in this data set than previous examples. The major factor in the degradation arises from the use of low elevation satellites and multipath contaminated differential corrections. The use of the range bias feedback option resulted in only minor differences in the final height solution (2-5 cm).

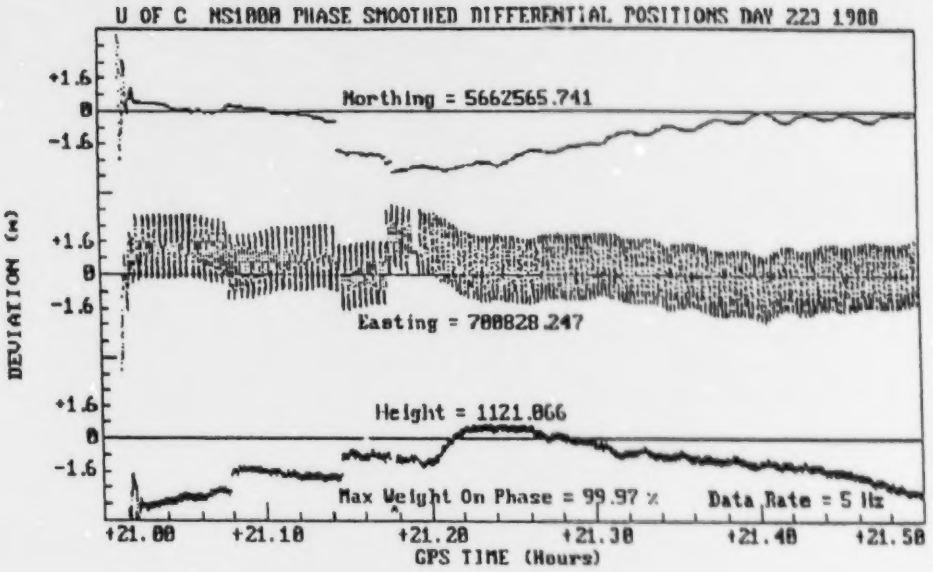

Figure 40. Day 223 Multi-Filter Kinematic Position Graph

The DRP method of phase processing was used to generate GPS positions for the oscillating mast with sufficient accuracy to provide meaningful position correlations at the centimetre level. The generation of GPS results was done assuming a common starting epoch which coincided with the vertical position of the mast and to the zero degree reading on the APR unit. Data decimation was not used for this analysis and both TI4100 P code and NS1000 C/A code data sets were processed.

Software was developed to aid in the post processing of raw APR data and analysis. The first program performed the decoding of the mast APR time and angle data and generated a formatted output APR position file. A second program, using the two sets of position data (adjusted APR and phase derived GPS positions), generated differences in northing, easting, and height coordinates and their associated statistics. To account for known systematic calibration corrections, various parameters were modeled into the computation of a time correlated position from the time correlated angle data. The APR position generation program therefore requires the following input information:

1. start time and end time in hours, min, and sec,

2. angular calibration value for zero degree offset,

3. angular lag value to correct for directional dependent slack in APR encoder drive and or GPS phase tracking loop lags,

4. time offset to correct for APR/GPS time synchronization errors (set to 0.0 sec),

5. mast orientation azimuth (89°, ±0.5°),

6. mast radius length in metres with antenna phase center offset added, and

7. WGS84 mast reference position coordinates for a mast position of zero degrees with no height correction for antenna phase center offset (cancels with monitor).

The variation of mast orientation angle was required to remove velocity correlated deviations in the northing coordinate differences, and was found to be insensitive (i.e. < 1 cm) to less than 1/2 degree changes. The time offset was held at zero since there was a high degree of confidence in the time tagging and initial testing showed an offset of greater than 250 msec was required to reduce velocity dependent errors. The initial position was then entered. Any slight height bias error in the position at the initial time, selected for the zero degree stationary position was removed (2-3 mm) by this entry and the angular calibration value.

Angular calibration and lag values were adjusted to minimize position deviations in the first few minutes of data. The calibration value (±2.5°) accounts for any errors in the zero degree setting of the APR. This calibration was done approximately during the experiment with a carpenters level while the mast was placed in a vertical position. The angular lag value was then adjusted to remove the major directional dependent errors which were most likely due to lags in the phase tracking filters within the GPS receiver. This error (±2.5°) was removed after all other adjustments were made and resulted in reducing residual errors from 10 to 20 cm down to the 5 cm level. There were however some small (2-5 cm) residual directional dependent errors due to the non-linear acceleration of the mast. Once the first 500 samples of position differences were calibrated the entire data period was processed.

Examinations of the following position difference graphs (Figures 41 to 43) indicate that residual random differences in Northing from 1 to 6 cm, Easting from 3.5 to 5.5 cm, and Height from 3.2 to 10.4 cm: all less than the 20 cm L1 frequency wave length. There are also some apparent systematic trends, especially in the height component on Day 224 (Figure 42), which are likely caused by phase measurement errors due to multipath, antenna phase center variation, and antenna imaging. Since Day 221 GPS DRP processing required a precise zero degree starting epoch for the mast and data was available only every 1.2 seconds, a significant starting position error is likely. This initial position error results in the systematic drift in position apparent in Figure 43.

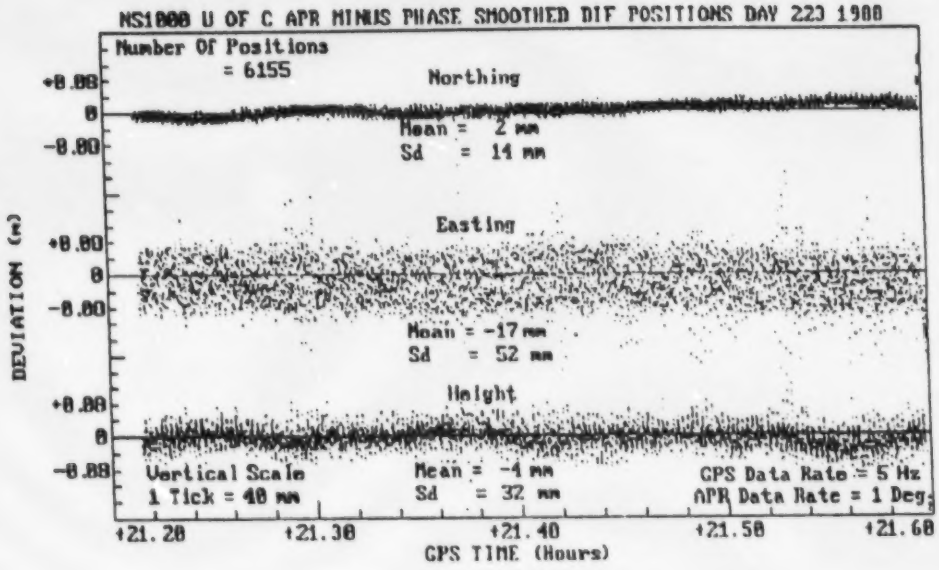

Figure 41. APR Minus GPS Position Difference Graph 100% Phase Day 223, 1988

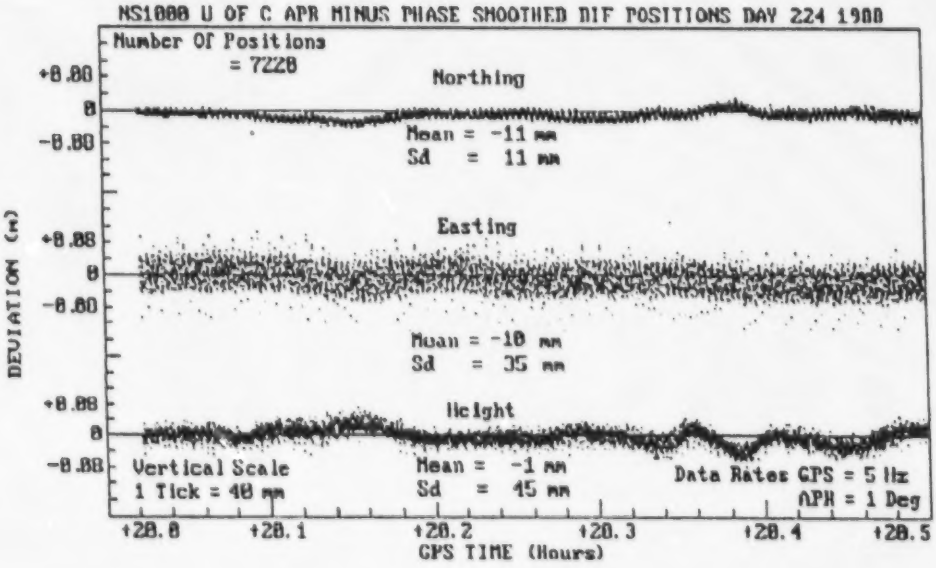

Figure 42. APR Minus GPS Position Difference Graph 100% Phase Day 224, 1988

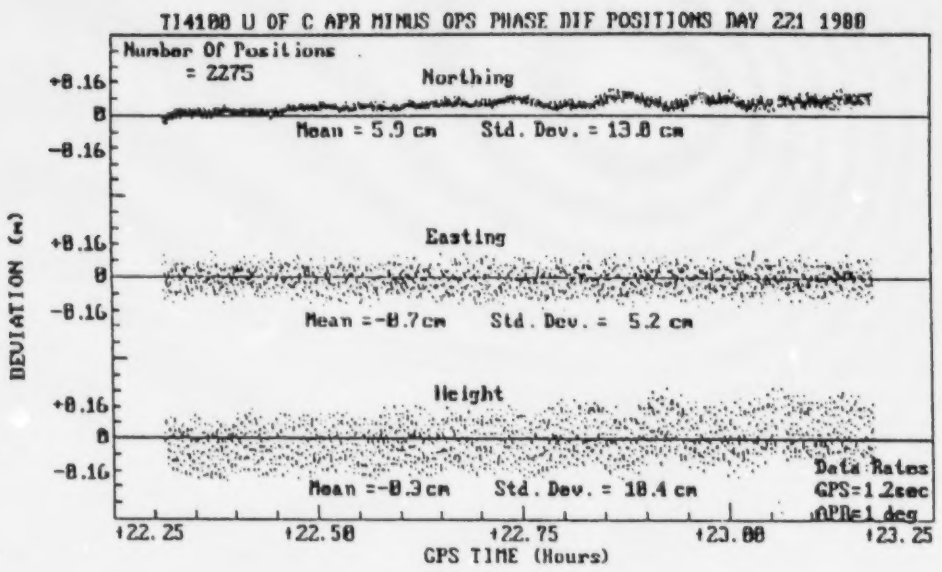

Figure 43. APR Minus GPS Position Difference Graph 100% Phase Day 221, 1988

The differences between TI4100 and NS1000 receiver results are not likely due to receiver phase tracking characteristics (i.e. phase tracking bandwidths were 8, 10, and 5 Hz for Days 221, 223, and 224 respectively). It is more reasonable to assume that a longer mast length (4.41 m) combined with a shorter oscillation period of 8 seconds on Day 223 would increase mast accelerations (± 1.5 m/sec^2) and result in a general increase in residual direction dependent lag errors in the easting coordinate (cf. Figure 44). The effect of increased mast length and angle (30°) also contributed to increased mast acceleration related error (bounce) and higher position difference noise levels on Day 221 (Figure 45). This mast height effect was however offset by a increase in the oscillation period to 20 seconds on Day 221, and peak accelerations were reduced to ± 80 cm/sec^2. Day 224 data (Figure 46) which used the shortest mast length (2.27 m), a 12 second period, and a 20 degree oscillation angle, provided the least amount of mast acceleration (-20 to +60 cm/sec^2).

The linear interpolation of APR positions, to matching GPS positions, introduced the next largest error in position differences, especially at the greater maximum swing angles (± 30°). This interpolation error was, however, limited in software by a 500 msec test to reject APR angles that were subject to delays (>1 sec) at the maximum angles corresponding to the end points of the swing arc. This delay arises from the fact that a change in angle of greater than one degree is required before a new APR angle observation is output (cf. Section 3.1.2). Large position

differences (>80 cm) are still present near the end of the swing arc due to the combined effects of phase measurement tracking errors arising from mast bounce accelerations and position interpolation errors which are more likely at the end of swing with NS1000 data due to its higher rate of output (cf. Figures 41 and 42).

Mast accelerations are not perfectly symmetric, due to mechanical deficiencies in the drive mechanism, but exhibit a very consistent signature from one period to the next. The three APR data graphs have acceleration peak times which correlate well to periods of zero degree mast angle and maximum mast velocity. Assuming a ship a sea would have a much smoother accelerations and a shorter maximum swing angle, similar if not better relative GPS kinematic positioning results should be achievable in shipborne applications.

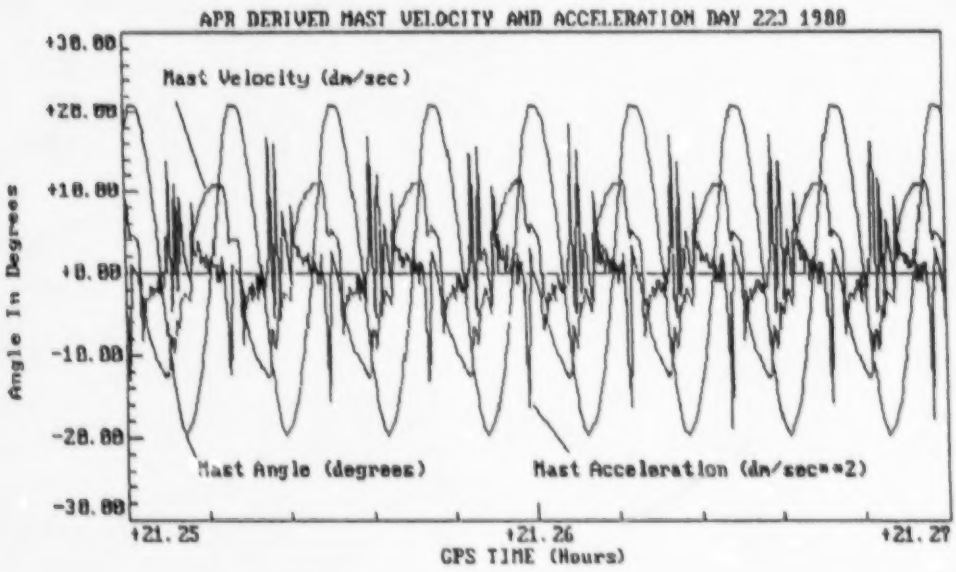

Figure 44. APR Angle Derived Mast Velocity and Accelerations Day 223

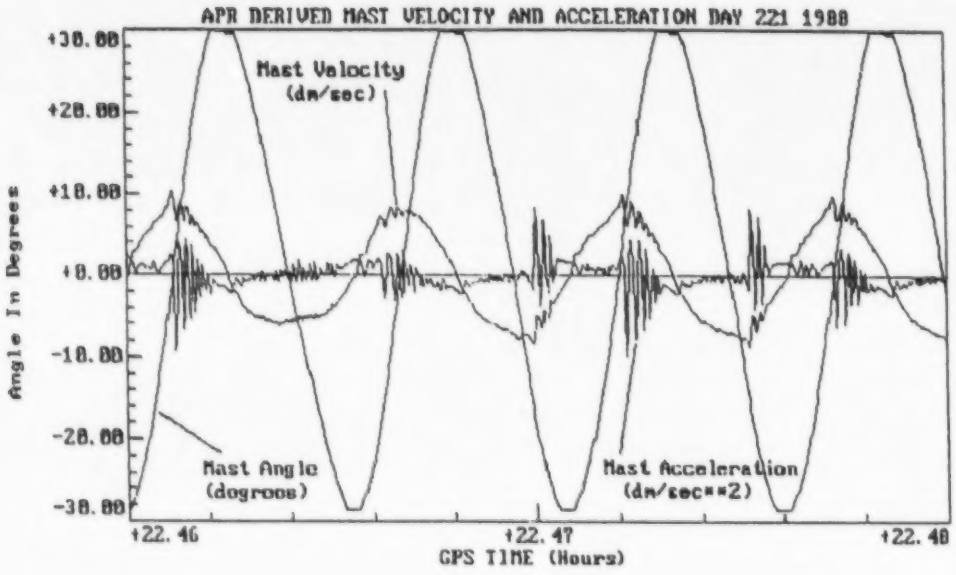

Figure 45. APR Angle Derived Mast Velocity and Accelerations Day 221

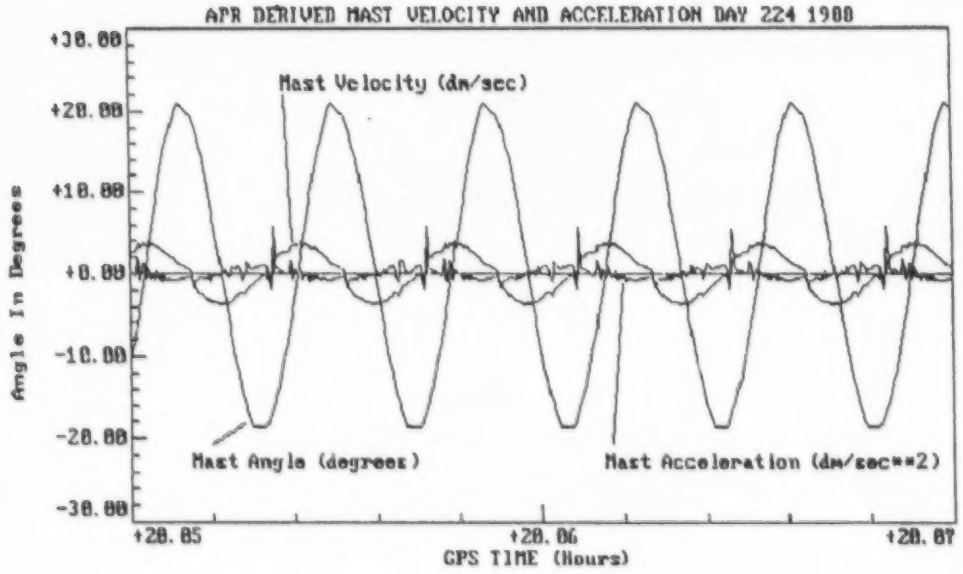

Figure 46. APR Angle Derived Mast Velocity and Accelerations Day 224

4.2. RF Absorbent Ground Plane Experiment Results

To better quantify the effects of monitor station pseudo range multipath errors, a special RF absorbent material ground plane was used to shield the antenna. Both P and C/A code pseudo range misclosures with corresponding phase smoothed ranges, were analyzed with and with out the antenna ground plane from the same monitor station position (HI = 1.308 m) used in the previous experiment. Figures 47 and 48 illustrate the dramatic decrease in systematic errors due to multipath for P code data collected from the same period. These deviations without the antenna ground plane correlate very well with previous monitor station differences (cf. Figure 14) taking into account the daily shift of 3 minutes and 56 seconds of the satellite constellation.

C/A code pseudo range noise results are also dramatically reduced by the addition of a ground plane as illustrated in Figures 49 and 50 . C/A code multipath is not, however, completely eliminated by the ground plane as indicated by the presence of minor multipath variations on satellite Prn 9 at 15.5 hours (Figure 50). Since only one day of C/A code ground plane data was collected, comparison of the same time period was not possible.

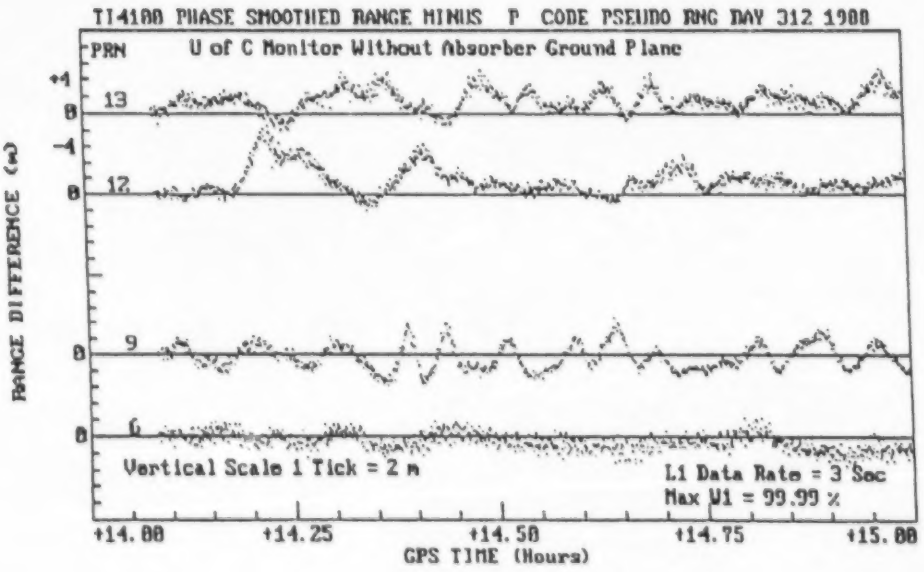

Figure 47. P Code Pseudorange Noise Graph Without Absorbent Ground Plane Day 312 14:00 - 15:00

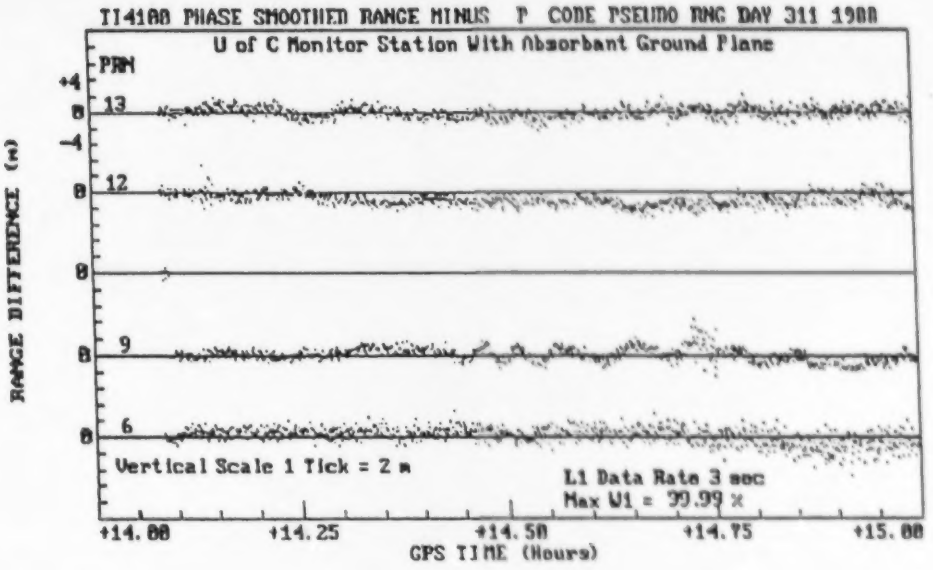

Figure 48. P Code Pseudorange Noise Graph <u>With</u> Absorbent Ground Plane Day 311 14:00 - 15:00

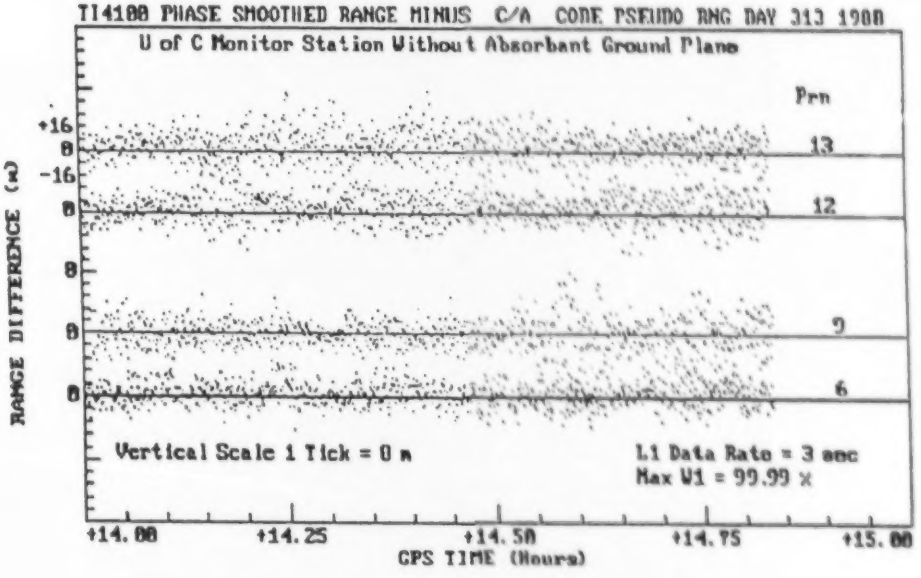

Figure 49. C/A Code Pseudorange Noise Graph <u>Without</u> Absorbent Ground Plane Day 313 14:00 - 15:00

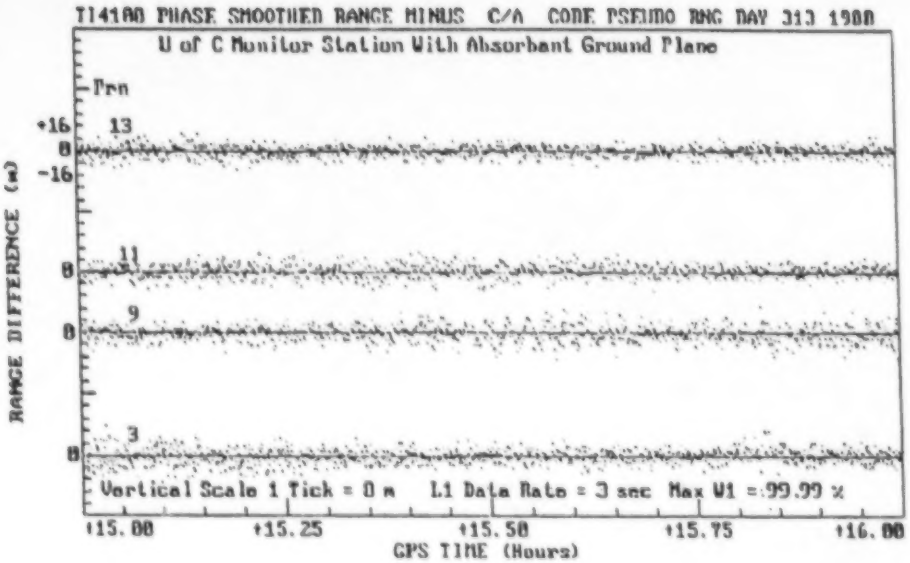

Figure 50. C/A Code Pseudorange Noise Graph <u>With</u> Absorbent Ground Plane Day 313 15:00 - 16:00

The results from the complete antenna ground plane experiment are summarized in Table 8. P code range standard deviations are very similar to those found in previous investigations with a reduction in rms noise levels of approximately 50 % with the use of the ground plane. C/A code pseudo range standard deviations indicate a similar reduction in multipath. The differences between TI4100 high multipath pseudo range noise levels (8 m) and previous NS1000 results (4-6 m) are attributable to the difference in data rates (i.e. 3 sec vs 200 msec). Low elevation biases, indicated in the table with a *, are due to the use of too high a phase weighting constant (99.99%) for generation of all the differences (cf. Figure 51). A complete set of graphs and individual satellite statistics which further illustrate the low elevation effect, are contained in Appendix F. MCAD filtering examples are also contained Appendix F which illustrate the effectiveness in filtering of C/A code range noise that is less influenced by multipath.

RF Ground Plane Experiment Pseudo Range Noise Statistical Summary

	PERIOD	CODE	SAMPLES	AVERAGE STD.DEV.	GROUND PLANE
November 6, 1988 Day 311					
1	13:00 14:00	P	4668	0.679	Y
2	14:00 15:00	P	4387	0.803	Y
3	15:00 16:00	P	4575	1.144	N
4	16:00 17:35	P	7121	1.499*	N
November 7, 1988 Day 312					
1	13:00 14:00	P	5562	1.306	N
2	14:00 15:00	P	4396	1.385	N
3	15:00 16:00	P	4258	0.665	Y
4	16:00 17:35	P	6924	1.272*	Y
November 8, 1988 Day 313					
1	13:00 14:00	C/A	5639	7.908	N
2	14:00 15:00	C/A	3998	8.707	N
3	15:00 16:00	C/A	4794	4.410	Y
4	16:00 17:18	C/A	5946	4.760	Y

* low satellite elevation induced bias

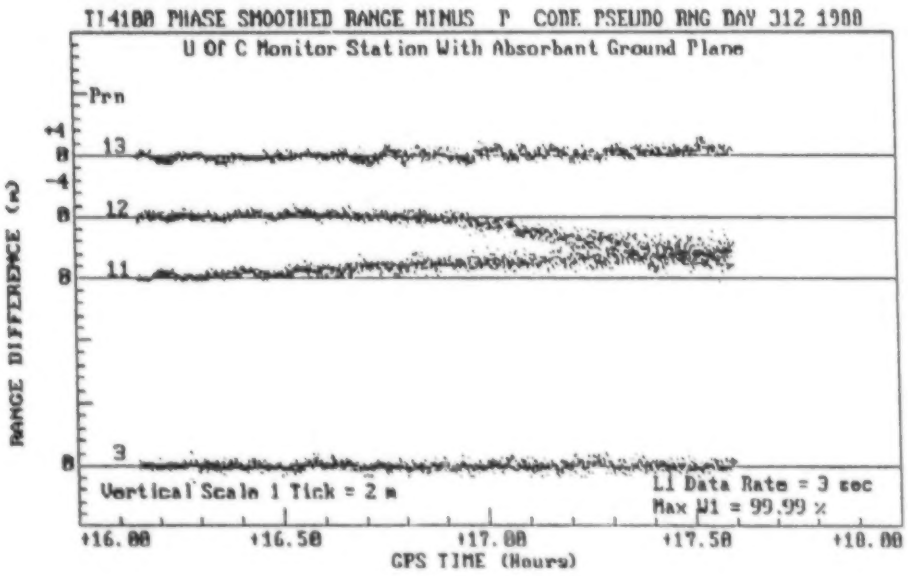

Figure 51. P Code Pseudorange Noise Graph With Absorbent Ground Plane Day 312 16:00 - 18:00

5. CONCLUSIONS AND RECOMMENDATIONS

The HYDROSTAR program enhancements were successfully completed and tested during the first phase of this contract. Major future additions are most likely to take place in the development of new receiver decoding modules and differential correction transmission formats suitable for a real time data link. Although the RTCM differential correction format has many advantages, its implementation should be carefully assessed according to the needs of the CHS and the ramifications of future GPS selective availability measures. Currently there are no alternative standards in place and if compatibility with future shore based systems and GPS receivers using RTCM standards is important, it is recommended that further development using the revised standard be undertaken.

A user clock constraint feedback technique was found to only have minimal effect (±5 cm) on the GPS position data since good 4 and 5 satellite geometry was available. Further testing under more adverse conditions may however prove this method to be beneficial during limited satellite coverage periods of poor GDOP. However, with future expansion of the GPS system to support a 21 plus 3 constellation, the number of satellites available for positioning will not be a major problem .Therefore it is recommended that further development and testing in this area not be supported.

Four methods of GPS multipath analysis were presented and using previous and current test data were found to be very effective. It was found in the analysis of the GPS pseudo range data that both C/A and P code multipath at a static monitor station have a significant effect on remote station positioning accuracies. Average peak multipath amplitudes were 20 m for C/A code ranges and 10 metres for P code ranges. FFT analysis of C/A code data proved to effective in removing high frequency noise and isolating low frequency multipath phenomena. Day to day correlations of filtered pseudo range variations at the various static sites were very strong indicating the validity of the methods presented.

Although phase smoothing removes a large percentage of the pseudo range multipath effect, initial filter convergence and cycle slips in the phase data combined with severe multipath may result in sizable differential correction errors (e.g. greater than 2 metres). These errors also result in a corresponding degradation in remote station positioning accuracies since the ranges are corrected using the erroneous differential corrections (e.g. greater than 10 metres depending on GDOP). Kinematic pseudo range data collected from the oscillating mast seemed to be relatively free of any major multipath effects confirming the assumption that antenna motion alleviates a majority of the multipath problem.

The technique of using multi-filters for pseudo range and phase measurement integration was demonstrated using both static and kinematic data sets. Code and phase GPS static and kinematic absolute positioning accuracies were less than 2.5 metres with much better short term relative kinematic results. Static results were not as good as kinematic results (±4m) due to the combined effects of static station code multipath contaminating the phase smoothed ranges. Using the multi-filter technique allows a higher weight to placed on the phase much sooner and guards against initial biases developing due to multipath contamination of the pseudo range measurements. This makes it possible to maintain smoother and more accurate differential corrections and improves remote position accuracies. Since the computational and storage overhead is minimal, its use is recommended for both monitor stations and shipborne remotes.

Using the discrete relative phase (DRP) method of positioning, static station position accuracies better than 10 cm were achieved with most of the errors attributable to multipath. Kinematic DRP positioning results, from three different days and two different receivers, were also better than 10 cm with most of the errors either due to monitor induced phase multipath errors or a combination of remote station phase measurement tracking loop lags and APR position interpolation errors. This analysis of phase data collected from both the stationary and kinematic GPS receivers confirms the assumption that multipath errors in phase measurements are much less of a problem than with pseudo range measurements. The DRP derived kinematic position accuracy estimates are also encouraging with respect to future development of sounding correction methodology using GPS phase data. Various methods of GPS roll, pitch and heave determination were outlined in Appendix D and it is recommended that further development and testing be undertaken.

The use of an RF absorbent ground plane during a second experiment proved to be very effective for reducing both P and C/A code static station multipath. It is therefore recommended to use a monitor station site free from obvious multipath sources such as: metal heating vents and other reflective structures such as towers and roof flashings, away from side slopes and embankments or cliffs, and as far away from water surfaces as possible. Failing this, efforts should be made to use a proper RF absorbent ground plane to shield the antenna from a majority of multipath. In any event multipath analysis of the monitor station GPS data should be conducted prior to any hydrographic surveys to ensure the quality of the differential corrections using a combination of the techniques developed under this contract.

Based on this report the recommendations for future research and development for a hydrographic GPS positioning system are as follows:

1. To further investigate RTCM differential correction transmission formats and perform verification of methodologies using field testing (shipborne remote preferable).

2. To develop the methods of GPS unaided and aided roll, pitch and heave determination using previously collected data and simulations. Future evaluation with a well designed shipborne test is also recommended.

3. To implement multipath detection methodologies for a monitor station analysis package and further investigate antenna ground plane multipath counter measures with different antenna designs.

4. To further develop kinematic phase positioning methodologies for practical application to hydrographic surveying.

Finally the development of better receivers with several more channels, higher data rates, and L2 phase measurements will have a profound effect on the future of GPS positioning. This combined with research and development efforts should result in a reliable GPS shipborne positioning system for all types of hydrographic surveying.

6. REFERENCES

BLAIS, J.A.R. AND A.A. VASSILIOU (1987), "Spectral Analysis of One Dimensional Data Sequences", UCSE Technical Report Number 30010, Department of Surveying Engineering, The University Of Calgary, Calgary, Alberta, Canada.

BRIGHAM, E.O. (1974), **"The Fast Fourier Transform"**, Prentice-Hall, Inc., Englewood Cliffs, N.J., U.S.A.

NORTECH (1986), "Phase 1B Report On Development Of Techniques Of Using GPS At Sea For Hydrographic Surveying", Report Prepared For The Canadian Hydrographic Service Under DSS Contract, File Number 50SS.FP901-5-R531.

NORTECH (1987), "Final Report On Development Of Techniques Of Using GPS At Sea For Hydrographic Surveying", Report Prepared For The Canadian Hydrographic Service Under DSS Contract, File Number 50SS.FP901-5-R531.

TRANQUILLA, J.M. AND B.G. COLPITTS (1988), "Investigation Into The Use Of Absorber Material For Multipath Control In GPS Antennas", A paper submitted for publication to **Navigation**.